UNIVERSITY OF VAASA

FACULTY OF TECHNOLOGY

ENERGY TECHNOLOGY

Ville Kumlander

DECOUPLING OF ELECTRICITY AND HEAT PRODUCTION IN ENGINE DRIVEN CHP PLANT WITH ENERGY STORAGE SOLUTIONS

Master´s thesis for the degree of Master of Science in Technology submitted for inspection, Vaasa, 31 October, 2016.

Supervisor: Professor Seppo Niemi

Instructor: Professor Kimmo Kauhaniemi

FOREWORD

This thesis was carried out within the research program Flexible Energy Systems - FLEX^{e}. The aim of this thesis was to study possibilities to decouple electricity and heat production in an engine driven CHP plant with energy storage solutions.

I express my gratitude to Kimmo Kauhaniemi who guided and instructed me through this project. Many thanks to Ville Kallioniemi in Wärtsilä Finland for providing me valuable information and material. I would like to thank Seppo Niemi for his informed comments as a supervisor. Jukka Rinta-Luoma may consider himself greatly thanked for letting me know about this project in the beginning of the present year. I would like to thank my parents, Juhani and Arja, for the tremendous support and cheers during my studies.

Vaasa, 31 October, 2016

Ville Kumlander

TABLE OF CONTENTS **page**

SYMBOLS AND ABBREVIATIONS

Symbols

c	specific heat capacity (J/(kg*K))
E	energy (Wh)
I	current (A)
m	mass (kg)
P	power (W)
T	temperature (°C)
U	voltage (V)

Abbreviations

CAC	charge air cooler
CHP	combined heat and power
DH	district heating
FLEX^{e}	Flexible Energy Systems
HT	high temperature
ICE	internal combustion engine
IRENA	International Renewable Energy Agency
$LiCoO_2$	lithium cobalt oxide
$LiPF_6$	lithium hexafluorophosphate
LT	low temperature
SOC	state of charge
VTT	Technical Research Centre of Finland

UNIVERSITY OF VAASA
Faculty of technology
Author: Ville Kumlander
Topic of the Thesis: Decoupling of electricity and heat production in engine driven CHP plant with energy storage solutions
Supervisor: Professor Seppo Niemi
Instructor: Professor Kimmo Kauhaniemi
Degree: Master of Science in Technology
Degree Programme: Degree Programme in Electrical and Energy Engineering
Major of Subject: Energy Technology
Year of Entering the University: 2011
Year of Completing the Thesis: 2016 **Pages: 61**

ABSTRACT

An engine driven CHP plant offers a high efficiency choice for district heating applications and electricity production. The plant is able to start and stop within minutes so it operates well in a system with increasing share of renewables. Heat production utilizes engine cooling and exhaust gases so it does not have an effect on electricity production. Flexibility enables the plant to run during high electricity prices and to be idle during low: a heat storage is able to meet heat demand during unprofitable times.

The aim of this thesis was to study possibilities for decoupling of heat and electricity production in an engine driven CHP plant with energy storage solutions. A Simulink model was constructed to simulate the operation of a plant which consisted of one Wärtsilä 20V34SG gas engine and an energy storage. A steel tank and a lithium-ion battery was studied in the theory part of the thesis.

The simulation part of the thesis was divided into electric and heat modes. The electric mode simulated a lithium-ion battery in case of smoothing fluctuations in electricity demand. The engine was run with a fixed power output throughout the simulation. Four fixed outputs of 7.5, 8.0, 8.5 and 9.0 MW were selected and the battery capacity was scaled for every power output. The power output of 8.5 MW offered the smallest battery capacity. As a result, smoothing of electricity demand with an electric battery was rather expensive, not to mention to decouple the whole production.

The heat mode simulations compared heat accumulator volumes with three different running costs and two different heat demands. The running costs were 70, 80 and 90 €/MWh per electricity-MWh. The first heat demand illustrated the demand during winter and the second one during summer. The simulations showed that it was more economical to utilize smaller heat accumulator volumes in the winter than in the summer. The average electricity price and heat demand were lower in the summer than in the winter which affected on the optimal accumulator volumes.

KEYWORDS: engine driven CHP, decoupling of production, energy storage

VAASAN YLIOPISTO
Teknillinen tiedekunta
Tekijä: Ville Kumlander
Diplomityön nimi: Kaasumoottorikäyttöisen CHP-voimalan sähkön- ja lämmöntuotannon eriyttäminen energian varastointia hyödyntäen
Valvoja: Professori Seppo Niemi
Ohjaaja: Professori Kimmo Kauhaniemi
Tutkinto: Diplomi-insinööri
Koulutusohjelma: Sähkö- ja energiatekniikan koulutusohjelma
Suunta: Energiatekniikka
Opintojen aloitusvuosi: 2011
Diplomityön valmistumisvuosi: 2016 **Sivumäärä: 61**

TIIVISTELMÄ

Moottorikäyttöinen CHP-laitos tarjoaa hyötysuhteeltaan erittäin hyvän vaihtoehdon kaukolämpökäyttöön ja sähköntuotantoon. Laitos pystytään käynnistämään, kuormittamaan ja pysäyttämään muutamassa minuutissa, minkä ansiosta se soveltuu hyvin järjestelmään, jossa uusiutuvan energian osuus kasvaa. Lämmöntuotannossa käytetään hyväksi moottorin jäähdytystä ja pakokaasuja, joten lämmöntuotanto ei vaikuta sähkötehoon. Joustavuus mahdollistaa laitoksen käyttämisen sähköntuotantoon korkeiden sähkön hintojen aikana, vaikka lämpökuorma olisi pieni, sillä lämpö voidaan varastoida sopivaan energiavarastoon.

Tämän diplomityön tavoitteena oli tutkia mahdollisuuksia eriyttää kaasumoottorikäyttöisen CHP-laitoksen sähkön- ja lämmöntuotanto energian varastointimenetelmiä hyödyntäen. Eriyttämistä tutkittiin Simulink-mallilla, joka rakennettiin kuvaamaan voimalaitosta, joka koostui yhdestä Wärtsilä 20V34SG -kaasumoottorista ja energiavarastosta. Teoriaosuudessa energiavarastoista tutkittiin terässäiliötä ja litium-ioniakkua.

Simulointiosuus jaettiin sähkö- ja lämpömoodeihin. Sähkömoodi simuloi litium-ioniakulla toteutettavaa kysynnän vaihtelun tasaamista. Moottoria ajettiin simuloinnissa vakioteholla. Neljä eri tehotasoa valittiin (7,5, 8,0, 8,5, 9,0 MW), ja akkukapasiteetti mitoitettiin sopivaksi jokaiselle tehotasolle. Tehotaso 8,5 MW mahdollisti pienimmän kapasiteetin käytön. Johtopäätöksenä todettiin, että sähköakulla toteutettava kuorman tasaaminen on melko kallista, puhumattakaan tuotannon eriyttämisestä.

Lämpömoodin simuloinnit vertasivat lämpöakkukapasiteetteja tarkastelemalla kolmea eri käyttökustannusta ja kahta eri lämmönkulutusprofiilia. Käyttökustannukset olivat 70, 80 ja 90 €/MWh tuotettua sähköenergiaa kohden. Ensimmäinen kulutusprofiili kuvasi kysyntää talvella ja toinen kesällä. Simuloinnit osoittivat, että oli taloudellisempaa käyttää pienempää akkukokoa talvella kuin kesällä. Tähän vaikuttivat kesän halvempi sähkön hinta ja pienempi lämmön kysyntä.

AVAINSANAT: kaasumoottorikäyttöinen CHP-voimala, sähkön- ja lämmöntuotannon eriyttäminen, energiavarasto

1 INTRODUCTION

An engine driven combined heat and power (CHP) plant offers a high efficiency choice for district heating applications and electricity production. Engine driven CHP plants are able to start and stop within minutes so they operate well in a system with increasing share of renewables. Energy storage solutions, such as a heat accumulator, enables the decoupling of electricity and heat production. As a result, the plant can be run during the high electricity prices and the storage is able to meet the heat demand during the low prices.

This work was carried out within the research program Flexible Energy Systems (FLEX^e) and was supported by Tekes – the Finnish Funding Agency for Innovation. The aim of the FLEX^e was to create novel technological and business concepts enhancing the radical transition from the current energy systems towards sustainable systems. The FLEX^e consortium consisted of 17 industrial partners and 10 research organizations. The programme was coordinated by CLIC Innovation Ltd.

The aim of this thesis was to study possibilities for decoupling of electricity and heat production in an engine driven CHP plant by means of energy storage solutions. A Simulink model was constructed to simulate the operation of a CHP plant which consisted of one Wärtsilä 20V34SG gas engine and energy storages. The thesis compared heat accumulator volumes at different operation methods, running costs and heat demands. A lithium-ion battery was studied in case of smoothing fluctuations in electricity demand.

Chapter 2 introduces the engine driven CHP plant and a district heating (DH) network. The chapter explains how DH water circulates in the plant. Short introduction is also made for electricity production and an electricity grid. Chapter 3 introduces energy storage solutions dealt with in this thesis. A stand-alone, stratified steel tank is explained and the basic principle of a lithium-ion battery is introduced. Chapter 4 presents the simulation cases which include electric and heat modes. The electric mode includes the electric battery simulations. The heat mode simulations evaluate the operation of the plant

with a heat accumulator. In Chapter 5, the simulation model is introduced. MATLAB and Simulink were used to carry out the simulations. The results from the simulations are found in Chapter 6 and Chapter 7 concludes the work. The summary can be found in Chapter 8.

2 ENGINE DRIVEN CHP PLANT

An engine driven CHP plant consists of one or more generating sets. One generating set includes an internal combustion engine (ICE), a generator and a heat recovery system. The heat recovery is based on hot water system and steam systems are not needed. In addition, the heat recovery is a hang-on type, meaning that recovering heat does not have an effect on performance of the engine. (Haga, Kortela & Ahnger 2012: 10.) Heat recovered from the engine is transferred to district heating water and directed to a customer. Electricity production is carried out with a generator connected to an electricity grid.

In this thesis, a Wärtsilä 20V34SG gas engine was under evaluation because it is the most suitable engine type for district heating applications. W20V34SG gas engines (Figure 1) are in CHP use, for example, in Denmark, Hungary and Italy. (Wärtsilä 2016a: 3, 4.)

Figure 1. Wärtsilä 20V34SG engine and alternator (Wärtsilä 2016b: 1).

The engine has 20 cylinders in V-configuration and with a cylinder bore of 340 mm. The piston stroke is 400 mm, the speed in a 50 Hz network is 750 rpm and the mean piston speed is approximately 10 m/s. The brake mean effective pressure is 22 bars. (Wärtsilä 2016b: 1.)

2.1 Heat production and district heating network

Various heat sources of an ICE can be utilized for heating DH water. Figure 2 illustrates how DH water circulates in the plant.

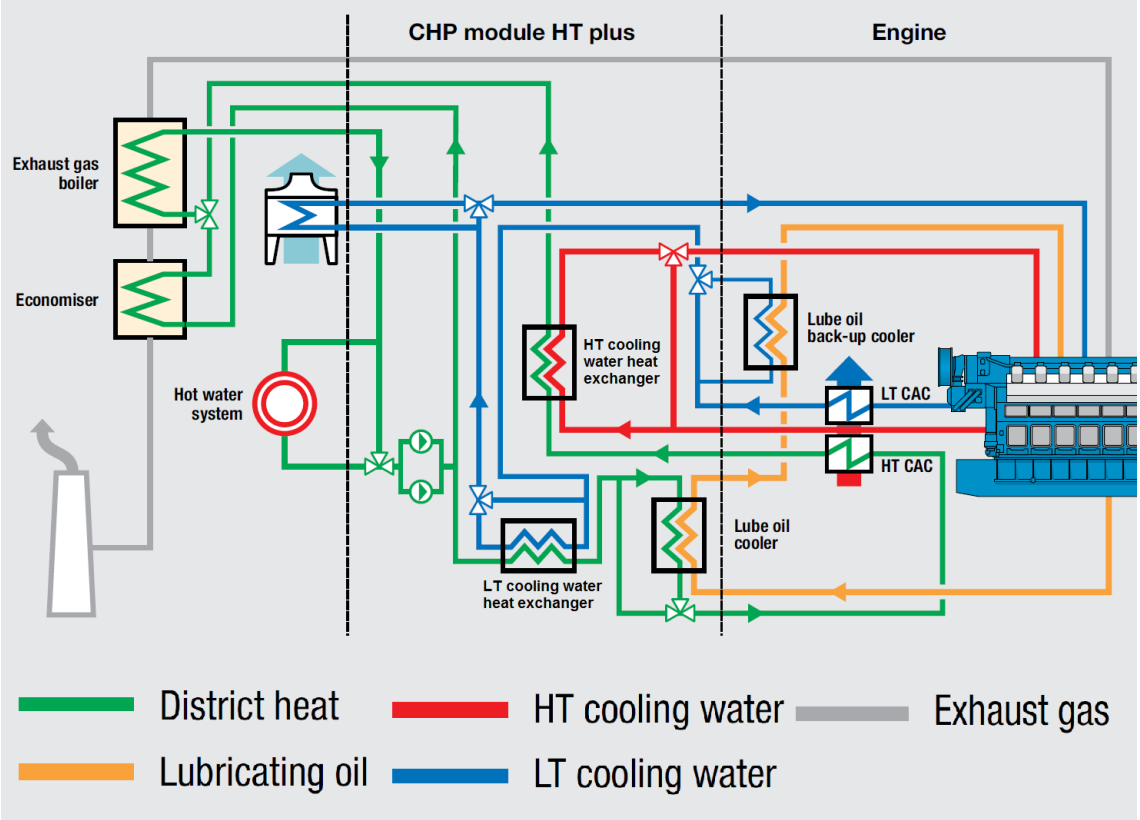

Figure 2. Layout of an ICE CHP plant (Modified from: Wärtsilä 2013: 7).

Six different heat sources can be used to heat DH water. At first, returning DH water from a customer flows through the low temperature (LT) cooling water heat exchanger. After this, water passes through the lube oil cooler. Raising the temperature of the lubrication oil will have a minor boost in electrical efficiency and it promotes utilization of lube oil heat. DH water is circulated through the high temperature charge air cooler (HT CAC) or, in conventional models, heat is transferred from a HT CAC to DH water with a heat exchanger. Before entering into the exhaust gas boiler and the economizer, DH water flows through the HT cooling water heat exchanger. (Wärtsilä 2016a: 4.)

The last and most effective heat transfer occurs with the interaction between DH water and exhaust gases (Huhtinen, Korhonen, Pimiä & Urpalainen 2013: 198). Wärtsilä (2013: 4) categorizes these components into economizers and boilers. The economizer is placed after the boiler and thus it operates at a lower temperature than the boiler. Boiler types can be divided into two groups: water tube and smoke tube boilers. In the smoke tube boilers, exhaust gas passes through pipes surrounded by water. In contrast, water circulates in pipes surrounded by exhaust gas in the water tube boilers. (Wärtsilä 2016a: 4.)

Engine power plants as well as other CHP plants are just a part of a district heating network. DH water can also be heated in district heating centers which are purely made for heat purposes. District heat is transferred to a costumer via a double pipe network in Finland: one pipe for supply water at the temperature of 65–120 °C and one for return water at the temperature of 40–60 °C. A DH pipe network is placed in the ground, approximately 0.5–1 m below streets, walking paths and park areas. (Energiateollisuus 2016a.)

DH water releases heat to a heating system of a customer through heat exchangers. This means that DH water never leaves the DH network and separate fluids circulates in customers' systems. Mechanical impurities, oxygen and other gases are removed from DH water to protect systems against corrosion and blocks (Energiateollisuus 2006: 44).

2.2 Electricity production and grid

Electricity is produced with a generator coupled to an engine via a flywheel and a coupling. Without a turbogenerator, the Wärtsilä 20V34SG gas engine produces 9 810 kW electric power at a frequency of 50 Hz. With turbogenerator the power is 9 930 kW. (Wärtsilä 2016b: 1.) In this thesis, the plant was examined without an optional turbogenerator.

The power system in Finland consists of three different power grids according to voltage levels: nation-wide transmission grids of 400 kV and 220 kV, regional networks of 110 kV and distribution networks between 0.4 kV and 110 kV. However, some exceptions occur in categorizing grids and networks. Power plants are connected to a grid or a network which has the most appropriate voltage level for them. (Fingrid 2016a.)

Prices in the Finnish electricity market are controlled by Nord Pool. Nord Pool is a power market offering trading, settlement and associated services in day-ahead and intraday electricity markets. Finland is a part of the markets and the electricity price is determined by the balance between demand and supply. In this thesis, Spot prices in Finland were used. Spot prices are day-ahead prices and they have been settled for every hour in the next day. (Nord Pool 2016.)

3 ENERGY STORAGE SOLUTIONS

Decoupling of electricity and heat production is possible with energy storage solutions. For example, heat energy can be stored in a thermal energy storage during high electricity prices and it can be released when it is not profitable to run the engine or when the heat demand is higher relative to thermal output of the engine running according to the electricity demand. The aim of this chapter is to introduce the theory behind a thermal energy storage and an electric battery.

3.1 Heat accumulator

A thermal energy storage offers various advantages for an efficient and flexible CHP plant usage. Firstly, it offers a solution to decouple the production. Secondly, the need for peak-load boilers is decreased and thus emissions may be reduced. Thirdly, the heat storage works as a buffer in case of maintenance or sudden shut down of the CHP plant. (Energiateollisuus 2006: 384.)

Thermal energy storages can be divided into three different technologies: sensible heat storage, latent heat storage and thermo-chemical heat storage. The sensible heat storage is based on heating or cooling solid or liquid storage medium, for example water or molten salt. The latent heat storage utilizes phase changing medium, such as paraffin. The thermo-chemical storage method is based on different chemical reactions, for example adsorption. (IRENA 2013: 1.) The division can also be made for short and long term storages. Energiateollisuus (2006: 385) categorizes latent heat and thermo-chemical storage for long term storing. Sensible heat is categorized for short term storing.

In this thesis, a steel tank storage was under evaluation. The steel tank storage (Figure 3) is a stand-alone cylinder form tank which is normally constructed on the ground but it can also be partly or entirely constructed into the ground.

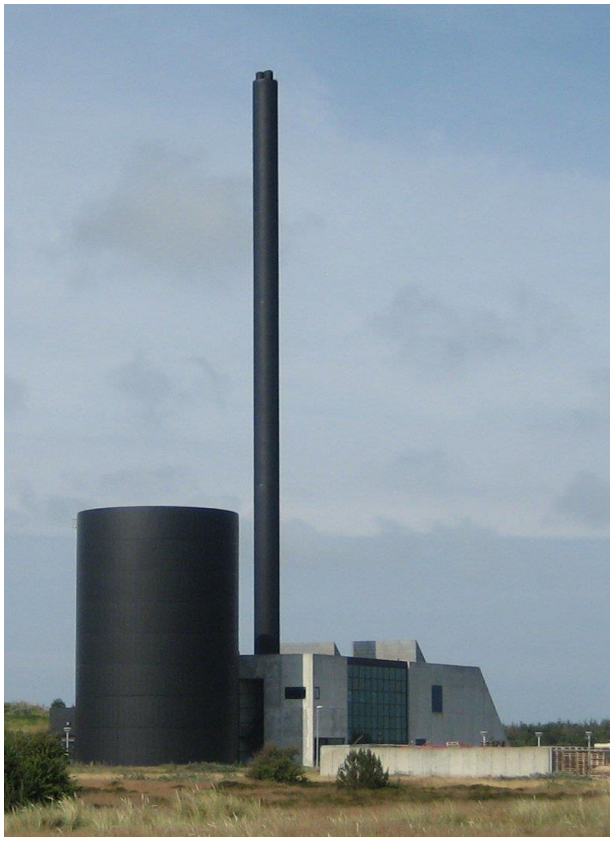

Figure 3. Skagen CHP plant in Denmark. The plant includes a heat accumulator (on the left) and three W28SG engines (Photo: http://skagensiden.dk/skagensiden/Nybyggeri/_Fotoasp/Img_2053.jpg).

Steel tanks can be divided into two different categories: unpressurized and pressurized. Unpressurized tanks store water at temperatures of below 100 °C and this type of tank was used for simulations in this thesis. Pressurized tanks are able to store water at temperatures of above 100 °C at a 0.5–2 bar gauge pressure. (Energiateollisuus 2006: 386.)

Heat required for temperature change in a material depends on the temperature change, the specific heat capacity and mass of the material. The quantity of heat stored in water can be calculated with the following equation

$$E = cm\Delta T, \tag{1}$$

where c is the specific heat capacity of water, m is mass of water according to the volume of the tank and ΔT is the temperature difference in the tank.

Water stratifies in the tank due to density difference (Figure 4). Hot water has lower density and hence it layers to the top of the tank. Cold water stratifies in the bottom of the tank. Between hot and cold water, a narrow mixed layer, called thermocline, occurs. It is desirable to keep the thermocline as narrow as possible and temperature gradient between hot and cold water as high as possible. Stratification is a sum of various matters. For example, the tank geometry, inlet and outlet port designs, fluid flow directions and operation conditions have an influence on how a narrow thermocline is formed. (Li 2016: 900.)

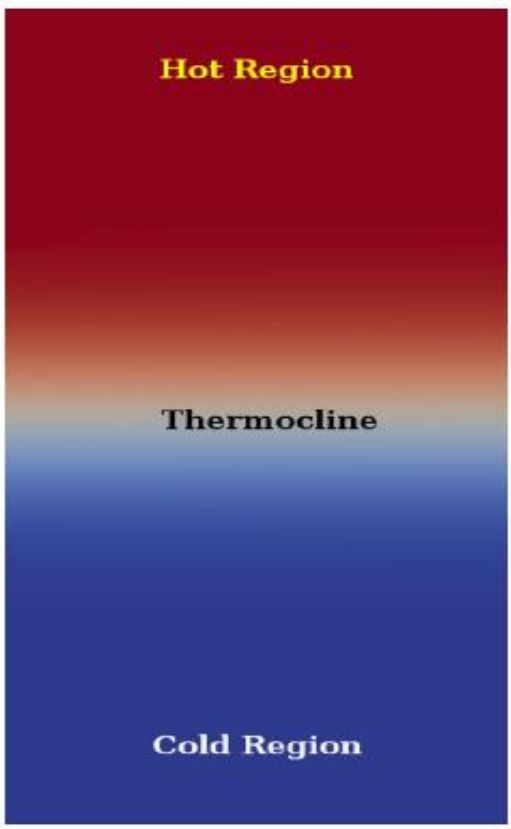

Figure 4. Stratification in a steel tank (Njoku, Ekechukwu & Onyegegbu 2016: 142).

Stratification increases the performance of a tank and it makes it possible to send water at a higher temperature to a consumer. Cold water is extracted from the bottom of the tank to cool down the engine (Campos Celador, Odriozola & Sala 2010: 3020). Stratification remains during charging and discharging of the tank (Figure 5).

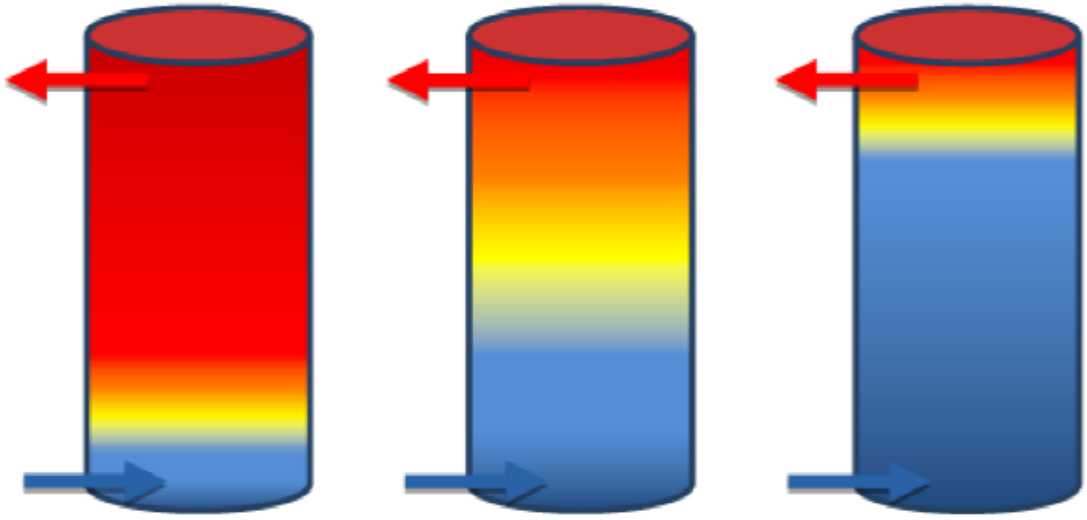

Figure 5. Stratification within a tank during discharge (Spanggaard & Schwaner 2013: 2).

3.2 Electric battery

IRENA, International Renewable Energy Agency, (2013: 5) divides batteries, dealt with in their report, into three different categories: low temperature (e.g. lithium-ion battery), high temperature (e.g. sodium-sulphur battery) and redox flow batteries (e.g. vanadium battery). Energy is stored chemically within these batteries. A lithium-ion battery was chosen for this thesis because of its high power and energy densities. These factors make the lithium-ion battery an ideal choice for applications requiring short discharge and high power performance. (IRENA 2015: 44.)

A lithium-ion battery (Figure 6) consists of two electrodes, an electrolyte and a separator (EPRI and DOE 2013: 96–97).

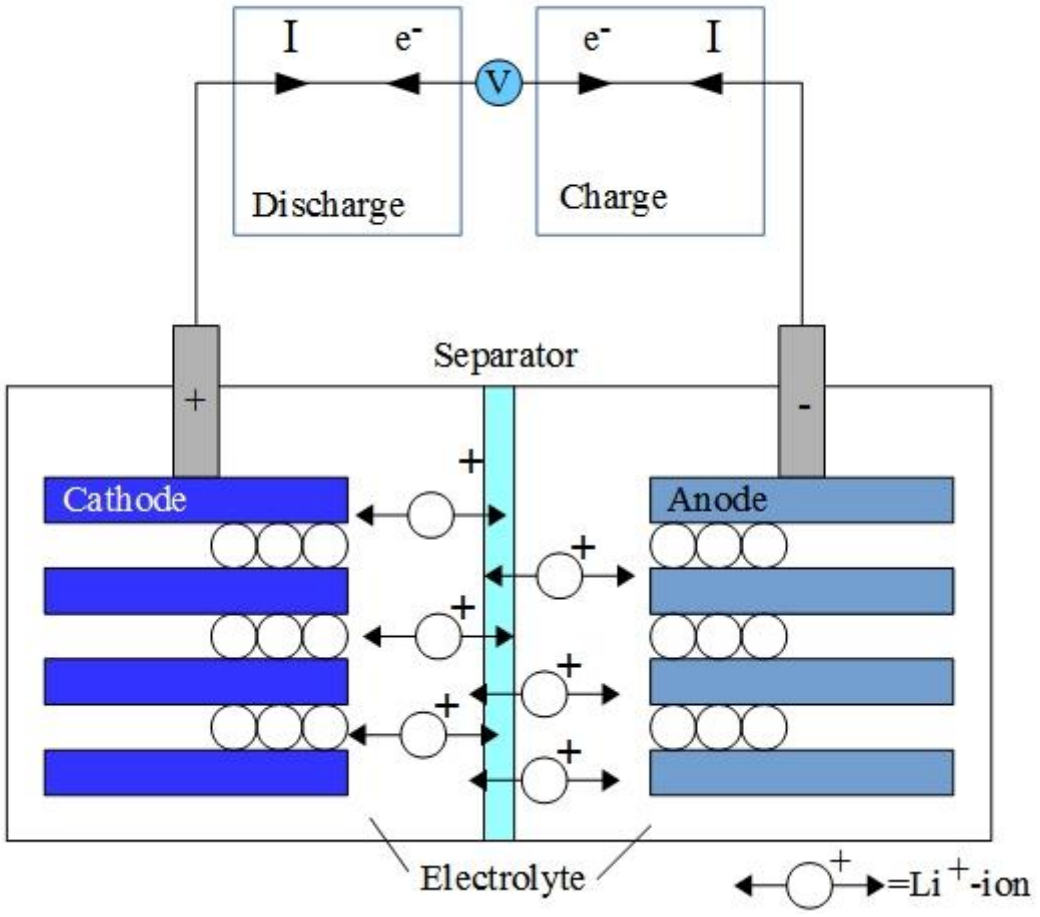

Figure 6. Layout of a lithium-ion battery (Modified from: EPRI and DOE: 97).

$LiCoO_2$, lithium cobalt oxide, is the most commercially utilized cathode material in lithium-ion batteries. Carbon as an anode material made the use of lithium-ion batteries possible two decades ago and is still widely used. (Nitta, Wu, Lee & Yushin 2015: 255, 260.) Organic solvents are the most common materials for electrolytes. Lithium hexafluorophosphate, $LiPF_6$, is the salt of choice for an electrolyte. It has an excellent conductivity and ability to form stable electrode passivation layers (Abraham, Furczon, Kang, Dees & Jansen 2008: 613). The purpose of an electrolyte is to ionically connect the cathode and anode. The separator, which is a porous insulating membrane, is needed to prevent electrons from moving side to side within the battery (EPRI and DOE 2013: 96–97).

Electrons are forced to move via an outer circuit hence giving power to a load. During discharge process, electrons flow from the anode to the cathode (Park, Zhang, Chung, Less & Sastry 2010: 7907). The flow is reverse during the charge process.

Figure 7 shows a containerized energy storage solution of Saft. It is a scalable megawatt-level electric energy storage and it can be transported wherever electricity is needed. Dimensions of the container are 6.1 m x 2.5 m x 2.9 m and it weights around 15 000 kg depending on the model (Saft 2015: 3–4).

Figure 7. Containerized electric energy storage of Saft (Photo: https://www.ny-best.org/sites/default/files/Saft.png).

4 PLANNING OF SIMULATION CASES

The results of this thesis are based on Simulink simulations. The simulations were divided into four different cases according to, whether electricity or heat production was prioritized. Electricity is a primary product in Case 1 and Cases 2–4 prioritize heat production. This chapter starts with an introduction to the electric mode simulation and Case 1. After that, Chapter 4.2 presents the plant operation when it prioritizes heat production. Cases 2–4 will be presented in the end of the chapter.

4.1 Electric mode - Case 1

Electricity was prioritized over heat production in Case 1. This kind of prioritization may exist in a situation where electricity demand needs to be secured all the time, for example under an isolation operation. If the demand is constant, the plant can run at a steady load, as well. However, if the demand varies, the output of the plant needs to follow the fluctuation in the demand. Another solution for this is to run the engine with a fixed power output and an electric battery takes the charge of smoothing the fluctuations in the electricity demand. The aim of Case 1 was to find a proper battery capacity to smooth the fluctuations in the electricity demand when the engine is driven at a fixed power output.

Heat production was not considered in Case 1 simulations while the focus was on the electric battery behavior. At a fixed output, the engine also produces heat at a constant power. The heat could be directed to a DH network or the engine could be cooled in conventional ways if there is no need for heat. In this case, it was assumed that the constant heat power produced by the plant is directed to a DH network. A simplified schema of the CHP plant with an electric battery and a district heating connection is shown in Figure 8.

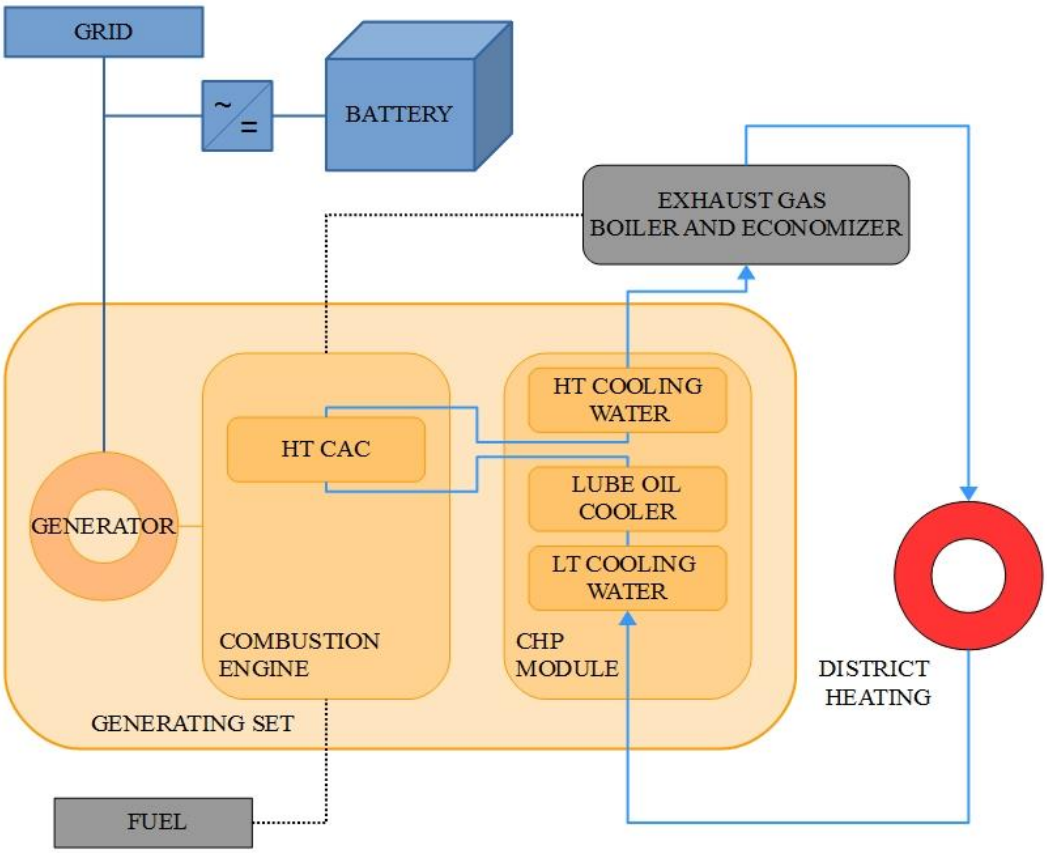

Figure 8. A simplified schema of the CHP plant with an electric battery.

The generating set includes an ICE, a CHP module, a generator, an exhaust gas economizer and a boiler and an electric battery connected to an electricity grid. The electric battery operates along with the engine and alternating current produced by the generator is rectified for the lithium-ion battery. The heat produced by the plant is directed to the DH network.

In the simulations, the engine and the battery were loaded with a varying electricity demand (Figure 9). The engine ran at a fixed power output and four outputs were selected: 7.5, 8.0, 8.5 and 9.0 MW. The target was to find a proper battery capacity for every fixed power output so that the battery would be able to store the excess energy and to respond to the changes in the demand. It should be noted that the capacity of the battery differed for every power output. Consequently, the results showed four different battery

capacities, one for each power output. The aim was to find the power output which offered the smallest battery capacity and the lowest price.

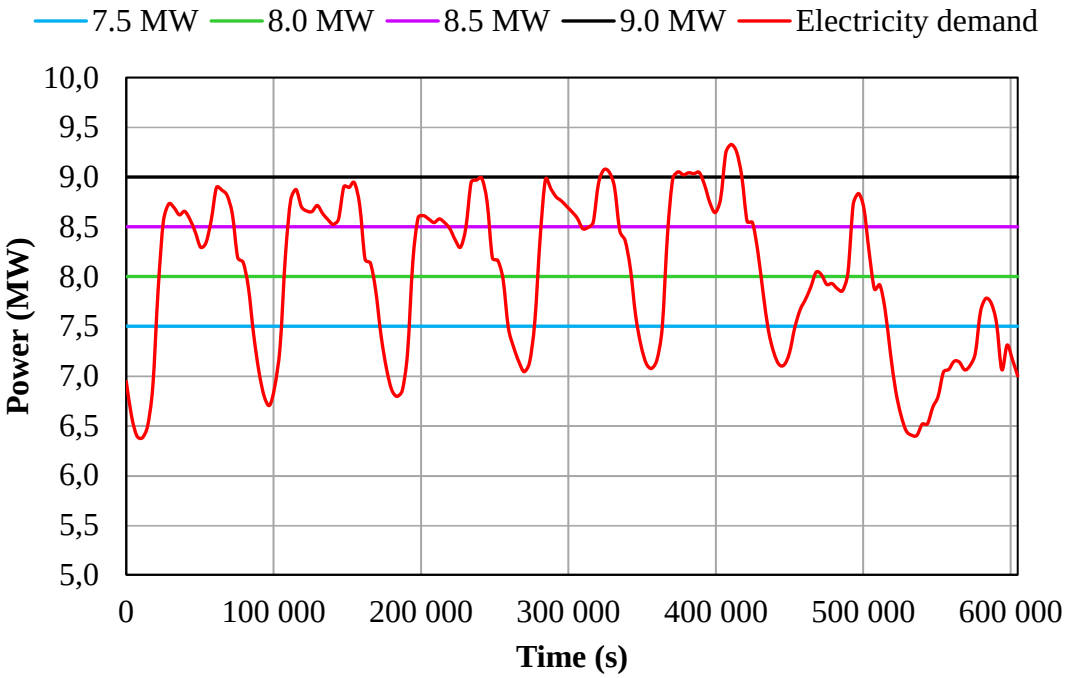

Figure 9. Electricity demand and engine power outputs in Case 1 (Fingrid 2016b).

The demand profile presents the variation in electricity demand throughout one week. It was scaled by using the real electricity demand in Finland (Fingrid 2016b). The time period is 604 800 seconds, i.e. one full week starting from Monday 0.00 o'clock. It should be noted that from Monday to Friday the peak loads are higher than those on Saturday and Sunday.

While the engine is running at a 7.5 MW power output, the demand is almost all the time higher than the engine output. Suitable battery capacity for this power output needs to fulfill the power deficit between the demand and output. On the other hand, for the power output of 9.0 MW, the battery needs to be able to store the excess energy while the engine output is almost constantly higher than the demand. Two remaining outputs, 8.0 and 8.5 MW, operate somewhere between these two above-mentioned situations. As a hypothesis, the outputs of 8.0 or 8.5 MW would result with the smallest battery capacity.

The maximum electric output of the model was 10 MW, so the engine ran at part loads in all simulations.

The battery parameters were scaled from Saft (2015: 4) IM+ Medium Power Plus battery. The appearance of the battery was introduced in Chapter 3.2. That battery has the capacity of 950 kWh and a maximum discharge power of 2 100 kW. The charge power was 1 000 kW, nominal voltage lied at approximately 700 V and the maximum current was 3 000 A. With this information, the battery parameters for the simulations in Case 1 were scaled and they are shown in Table 1.

Table 1. Parameters of the battery used in Case 1 simulation.

Discharge power	4 200	kW
Charge power	2 000	kW
Nominal voltage	1 400	V
Maximum discharge current	3 000	A
Maximum charge current	1 400	A

The simulation was conducted with the battery specification which could be achieved by placing two IM+ Medium Power Plus batteries in series. The maximum discharge current was not mentioned in the battery catalog and thus it was calculated with the following equation

$$I = \frac{P}{U} = \frac{2000*10^3\ W}{1400\ V} = 1428.57\ A = 1400\ A, \quad (2)$$

where P is the charge power and U is the nominal voltage of the battery.

4.2 Heat mode

The rest of the cases, Cases 2–4, have heat as the primary product and electricity as the secondary. Decoupling of energy production is carried out with a heat accumulator. The

aim of Cases 2–4 was to find out how the plant operates with different operation methods and heat accumulator capacities. The goal was to find the most suitable accumulator capacity for every case. A simplified schema of the CHP plant with a heat accumulator is presented in Figure 10.

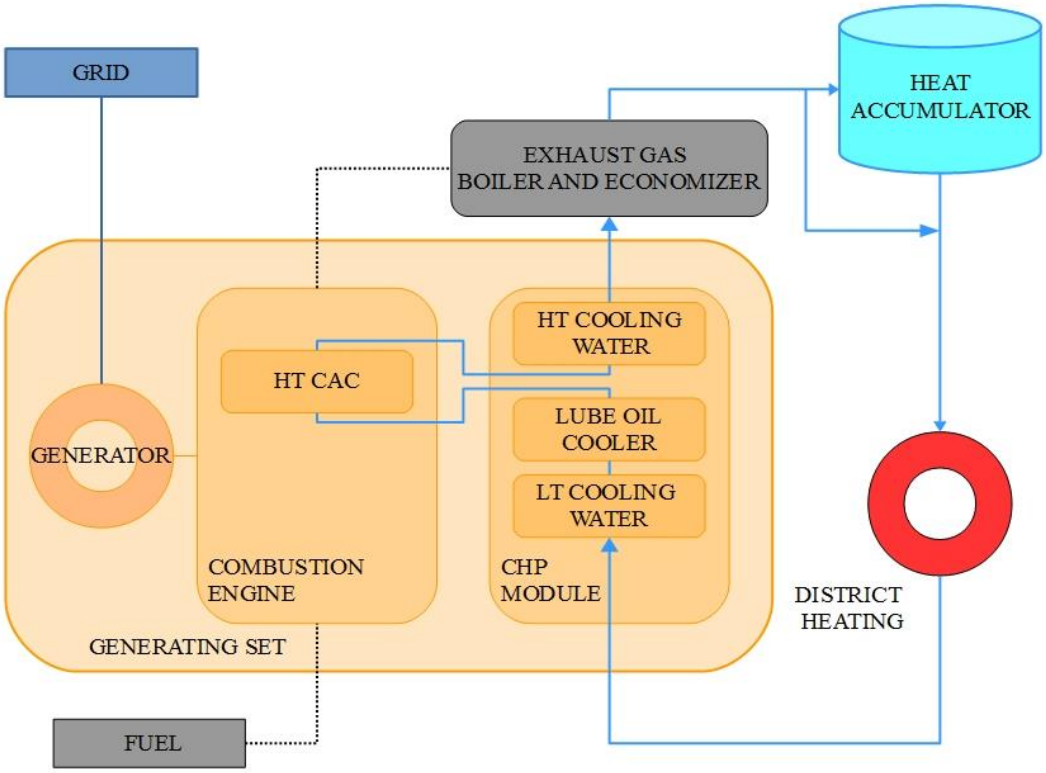

Figure 10. A simplified schema of the CHP plant with a heat accumulator.

The plant schema is the same as in the electric mode with the only exception that now there is a thermal energy storage. When the engine is running, hot water can be stored in the tank or it can be directed straight to the DH network. During the times the engine is shut down, only the heat accumulator feeds heat into the DH network.

4.2.1 Heat demand profiles

The heat mode cases are run according to two different heat demand profiles. These profiles present the heat variation during typical weeks in Finland: the first profile

illustrates the heat demand between 2nd and 8th February and the second profile between 22nd and 28th June. The profiles are created from the materials of VTT, Technical Research Centre of Finland. The materials of VTT included time series of heat consumption, outdoor temperature and time-of-day. The original material had heat consumption for different users according to their nominal heat consumption. A proper heat demand for this thesis was formed by adding users which had nominal heat consumption from 1 MW to 5 MW. The time period for all of the time series is 604 800 seconds, i.e. one full week starting from Monday 0.00 o'clock. The heat demand profiles and outdoor temperatures for February and June are shown in Figures 11–14.

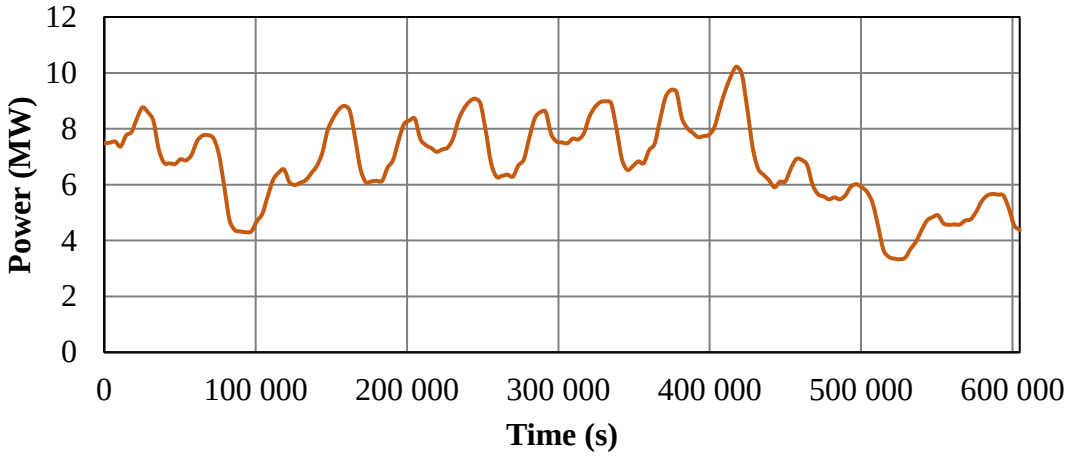

Figure 11. Heat demand from 2nd to 8th February.

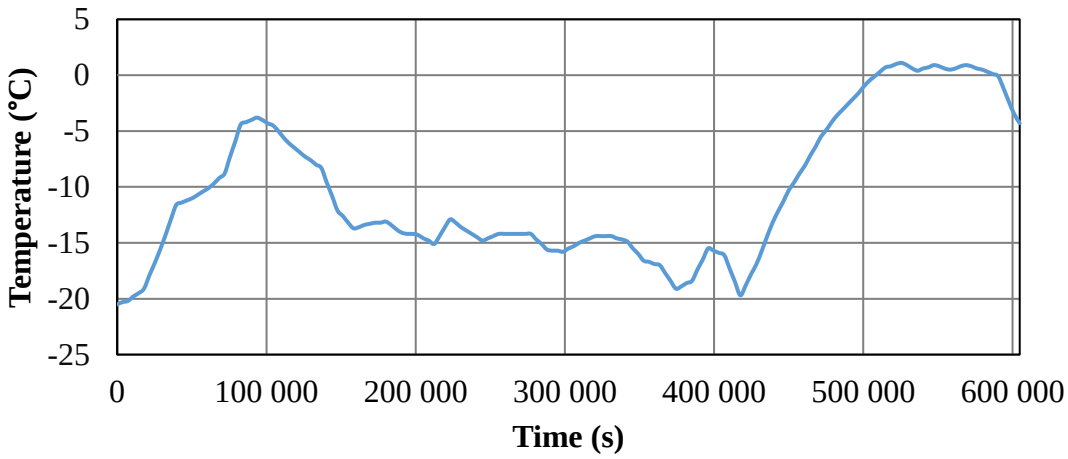

Figure 12. Outdoor temperature from 2nd to 8th February.

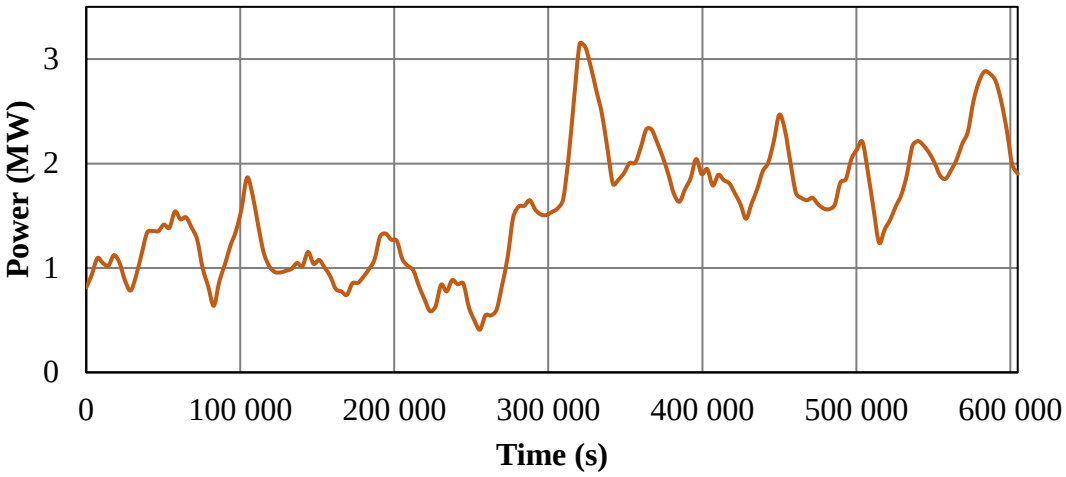

Figure 13. Heat demand from 22nd to 28th June.

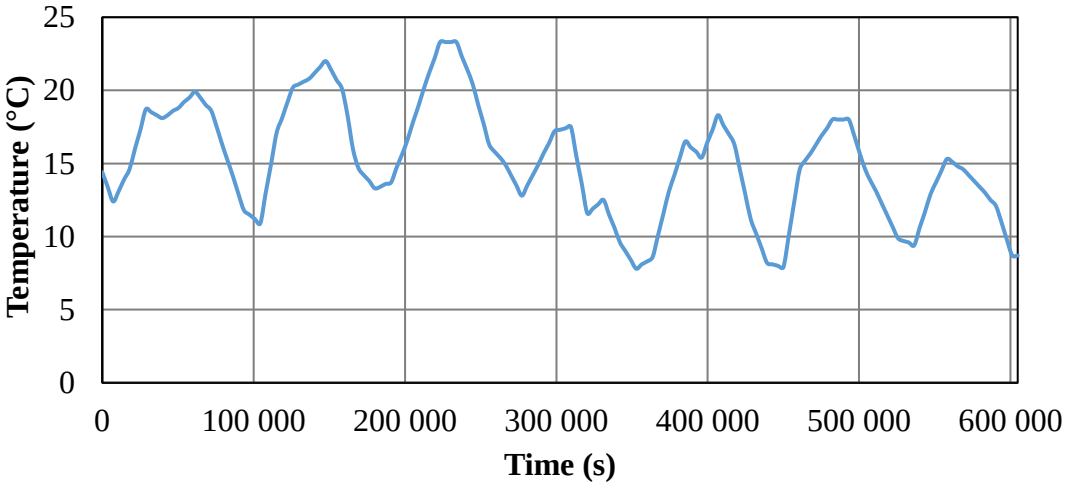

Figure 14. Outdoor temperature from 22nd to 28th June.

4.2.2 Profit and costs of the plant

The feasibility of the CHP plant was evaluated by comparing profit and costs. The income from the production of electricity and heat was taken into account. The economic examination did not take into account, for example, the income from customers to join the district heating network, taxes or emission fees. Nord Pool Spot prices from the year 2015 were used for the income of the electricity production. The prices for February and June are presented in Figures 15 and 16.

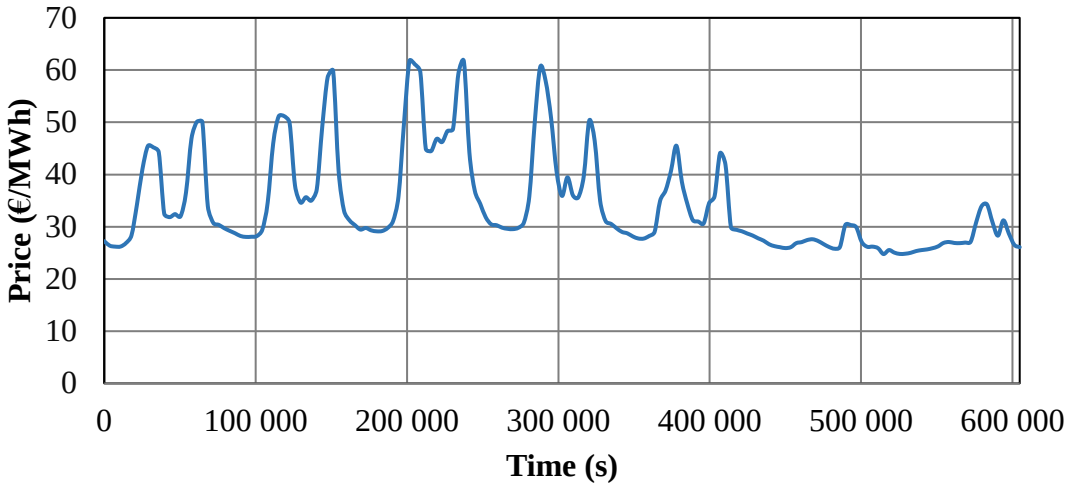

Figure 15. Nord Pool Spot price from 2nd to 8th February.

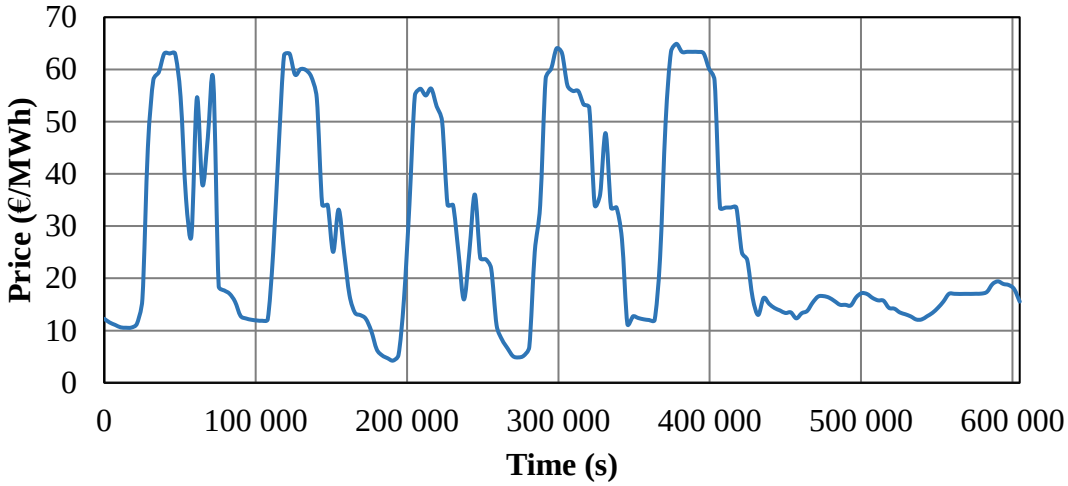

Figure 16. Nord Pool Spot price from 22nd to 28th June.

Heat price was approximately 71 €/MWh. This is the weighted average price for consumers whose annual heat consumption is approximately 600 MWh in Finland. For example, a block house consisting of 80 apartments with heat demand power of 230 kW has yearly heat consumption of around 600 MWh. (Energiateollisuus 2016b.)

Three different running costs of the electricity production were used in the simulations: 70, 80 and 90 €/MWh. These costs were per electricity-MWh. The values were based on

the information provided by Wärtsilä. The model observes the possible income from electricity and heat. The engine is started, if the income exceeds the running costs. If the income declines below the profitability limit, the engine is shut down. For example, when the running cost is 70 €/MWh, the current profitability limit is calculated with the following equation

$$profitability\ limit = 70\ \frac{€}{MWh} * \frac{10}{3600}\ \frac{MWh}{s} = 0.1944\ \frac{€}{s}, \tag{3}$$

where 10 MWh is the electricity production within one hour and 3 600 is the seconds within one hour. The current profitability limit for 80 €/MWh running costs is 0.22 €/s and for 90 €/MWh it is 0.25 €/s. The following Figure 17 presents the profitability limits for February.

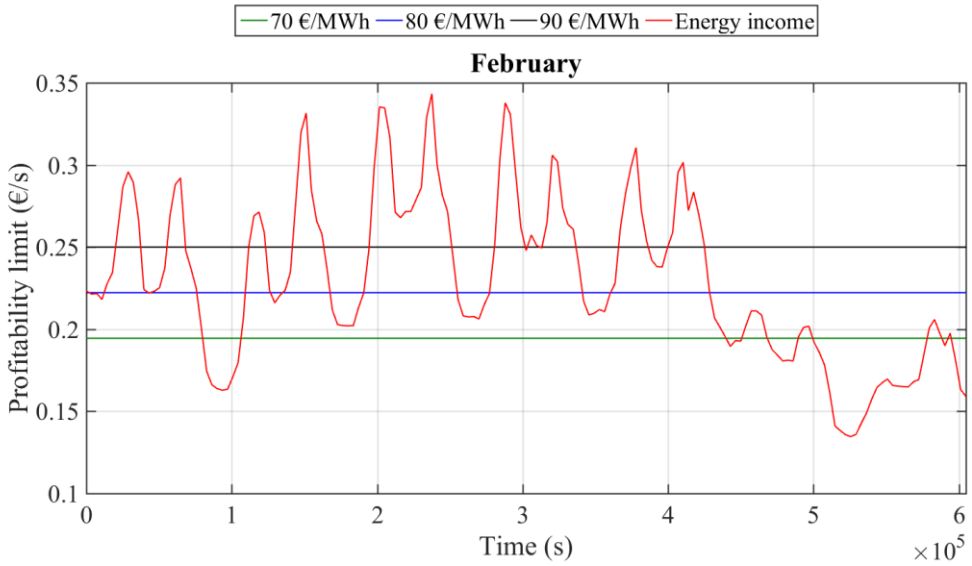

Figure 17. Profitability limits and possible income of the production in February.

The red curve indicates the sum of possible income from electricity and heat. When the red curve exceeds the required profitability limit, the engine is started. On the contrary, when the red curve drops below the required profitability limit, the engine is shut down. The following Figure 18 illustrates the profitability limits in June.

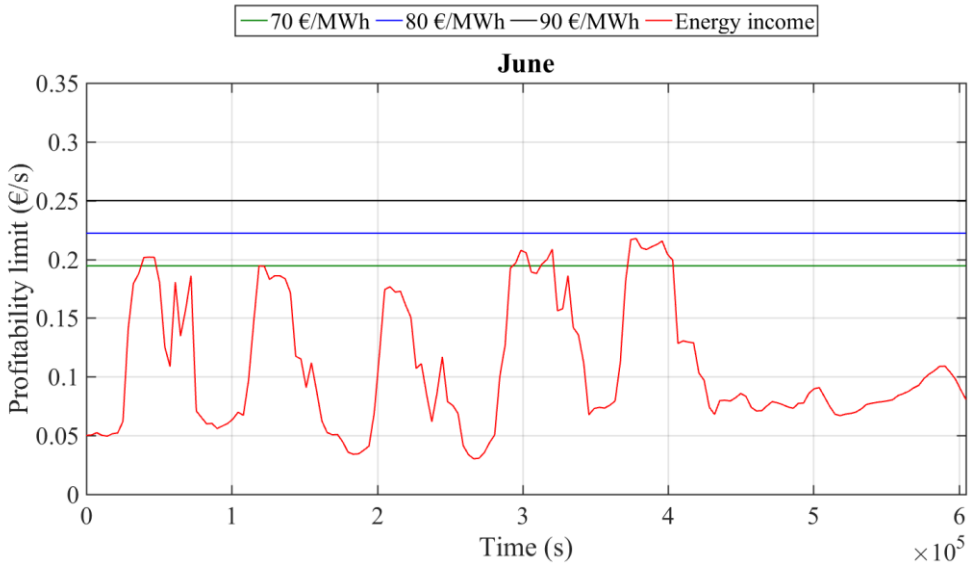

Figure 18. Profitability limits and possible income of the production in June.

The production is less economical in June than in February. This is because of the lower demand for heat in the summer season. Also, the average electricity price is lower in the summer than in the winter. The income from heat and electricity exceeds the current profitability limit only a few times at the running costs of 70 €/MWh and does not exceed the running costs of 80 and 90 €/MWh at any point in June.

4.2.3 Case 2 - Simple operation method

In Case 2, the plant has the simplest operation method out of all the cases including decoupling production with the heat accumulator. The operation method is illustrated in Figure 19. The figure depicts the stored energy, maximum and minimum capacities of the accumulator and the engine state whether it is running or not. In this case, the engine is only used to charge the accumulator. When the stored energy reaches the maximum capacity, the engine is shut down and the accumulator continues to respond to the heat demand. The minimum level for capacity is set at 5-% of the maximum value. When the stored energy lowers to the minimum level, the engine is started to recharge the accumulator. The simulation in Figure 19 was driven with the 800 m^3 heat accumulator and using the heat profile in February.

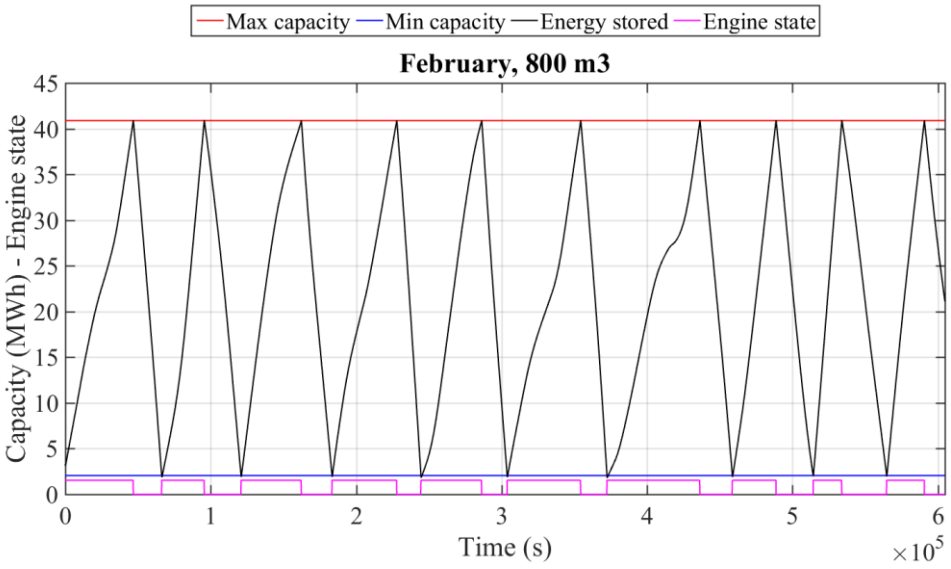

Figure 19. Graph of the simulation in Case 2.

4.2.4 Case 3 - Profitability limit

Case 3 includes a more advanced operation method than Case 2. The operation method is presented in Figure 20.

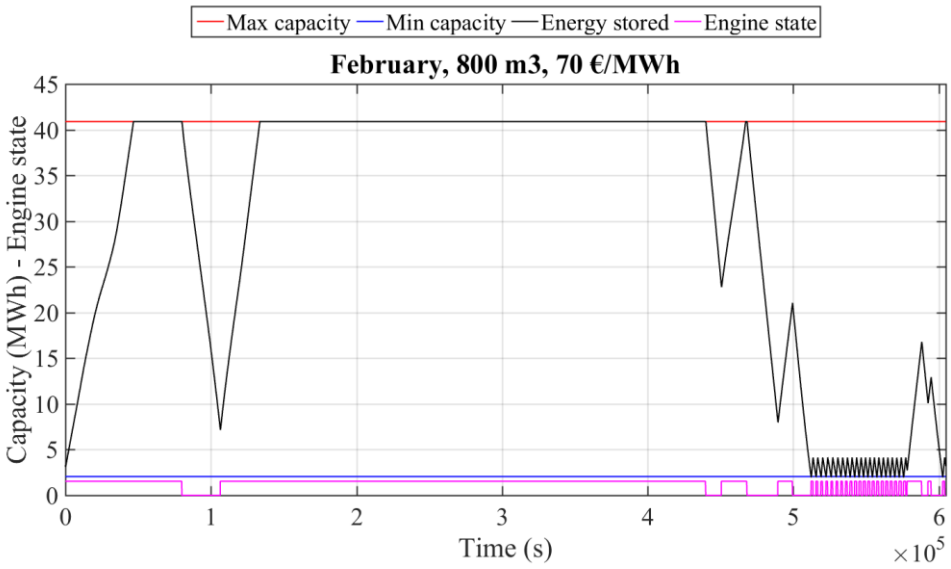

Figure 20. Graph of the simulation in Case 3.

Now, the profitability limit was introduced to the plant. When the income of the plant exceeds the production costs, the engine is started and it runs until the income drops below the production costs. When the engine is not running, i.e. running is not profitable, the heat accumulator responds to the heat demand. However, if the stored energy lowers to 5-% of the maximum value, the engine is started even though it is not profitable to run the engine. Then, stored energy is increased to 10-% of the maximum value regardless of the profitability limit. The simulation in Figure 20 was again carried out with the 800 m^3 heat accumulator and 70 €/MWh profitability limit based on the heat demand in February.

Case 3 also had a battery variant. The function of this variant is illustrated in Figure 21. The aim of this variant was to find a suitable electric battery capacity for balancing power output during the ramp-ups and -downs of the engine.

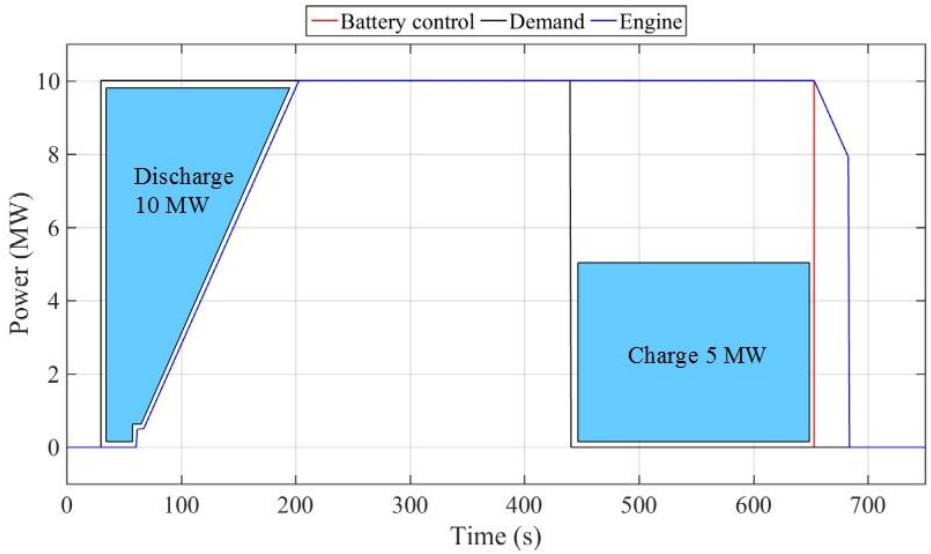

Figure 21. Discharging and charging of the battery in the battery variant of Case 3.

The battery is used to smooth the ramp-ups and -downs. When the engine is started, it takes some time for it to reach the maximum power output. The required power during the ramp-up is taken from the battery. This is illustrated in Figure 21 with the light blue triangle shape area on the left which takes place between 30 s and 203 s. Approximately at the time of 440 s, the demand drops from 10 MW to 0 MW. The engine continues to

charge the battery and it remains running until the state of charge (SOC) of the battery reaches 100-%. A SOC of 0-% means that the battery has no charge and 100-% is that it is fully charged. The battery is charged to its full capacity at the time 653 s and after this it takes 30 s for the engine to ramp-down and shut down. It should be borne in mind that the charge power is only approximately one half of the discharging power. The specification of the battery used in this variant is found in Table 2.

Table 2. The battery specifications in the battery variant in Case 3.

Discharge power	10 500	kW
Charge power	5 000	kW
Nominal voltage	3 500	V
Maximum discharge current	3 000	A
Maximum charge current	1 400	A

In comparison to Case 1, now the battery has more power but it is more likely to need to store less energy while it only has to manage ramp-ups and -downs.

4.2.5 Case 4 - Electric boiler

Case 4 is similar to Case 3 but now an electric boiler is added to the plant. An electric boiler converts electric energy into heat with an efficiency of 99-% (Garcia, Vatopoulos, Riekkola, Lopez & Olsen 2012: 14). An example of the operation in Case 4 is shown in Figure 22.

The electric boiler is used when the production costs exceed the income and stored energy in the accumulator has lowered to 5-% of the maximum value. In the figure, the green curve presents the state of the electric boiler. It shows that during the weekend when the electricity price is low, it is more advantageous to use the electric boiler. Simulation in Figure 22 was carried out with the 800 m^3 heat accumulator and 70 €/MWh production cost according to the heat demand in February.

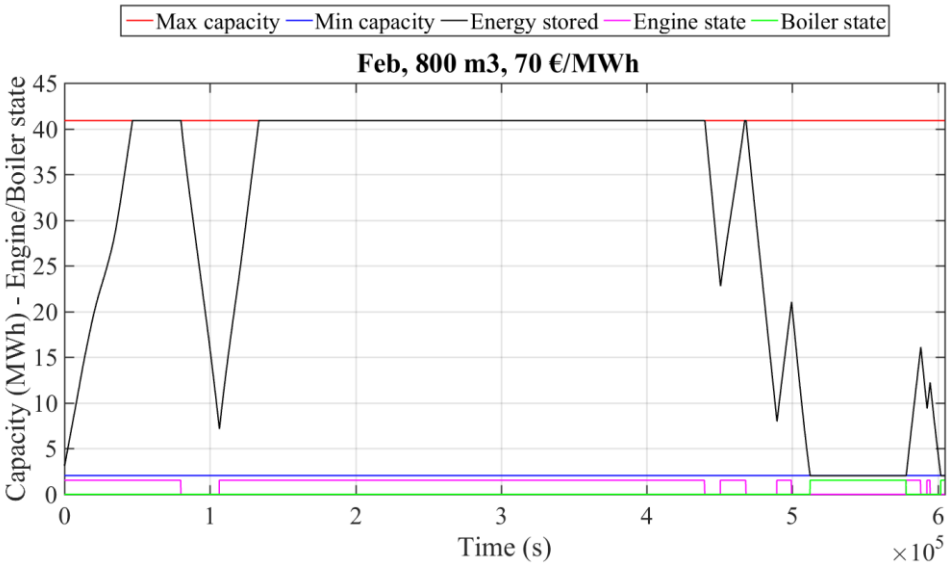

Figure 22. Graph of the simulation in Case 4.

Table 3 sums up all the simulation cases. The electric mode simulation consisted of Case 1. The aim of Case 1 was to scale a lithium-ion battery to smooth fluctuations in the electricity demand when the engine was driven with a fixed power output. The heat mode simulations included Cases 2, 3 and 4 and the aim of the simulations was to find optimal heat accumulator volumes. In Case 2, the engine was only used to charge the heat accumulator. In Case 3, the engine was started in two events: the profitability limit exceeded the running costs or the heat accumulator was drawn empty. In Case 4, the electric boiler heated district heating water when it was not profitable to run the engine and the heat accumulator was empty.

Table 3. The simulation cases.

Mode	Case	Primary product	Storage solution	Profitability limit	Electric boiler
Electric	1	Electricity	Electric battery		
Heat	2	Heat	Heat accumulator		
Heat	3	Heat	Heat accumulator	X	
Heat	4	Heat	Heat accumulator	X	X

5 SIMULATION MODEL

The simulations were performed with Simulink of MathWorks. Simulink offers a block diagram environment for simulation and model based design and it is integrated with MATLAB (MathWorks 2016). The aim of this chapter is to present the layout of the simulation models. Four different simulation models were constructed, one for each case. However, since the differences between the models were minor, only Case 1 and 2 are used as an example to describe the function of the models. The chapter starts with an introduction to the top layer model and the engine model. The heat accumulator is described after that and the electric battery model is introduced in the end.

5.1 Top layer

The top layer of the models reveals the information board and control features (Figure 23).

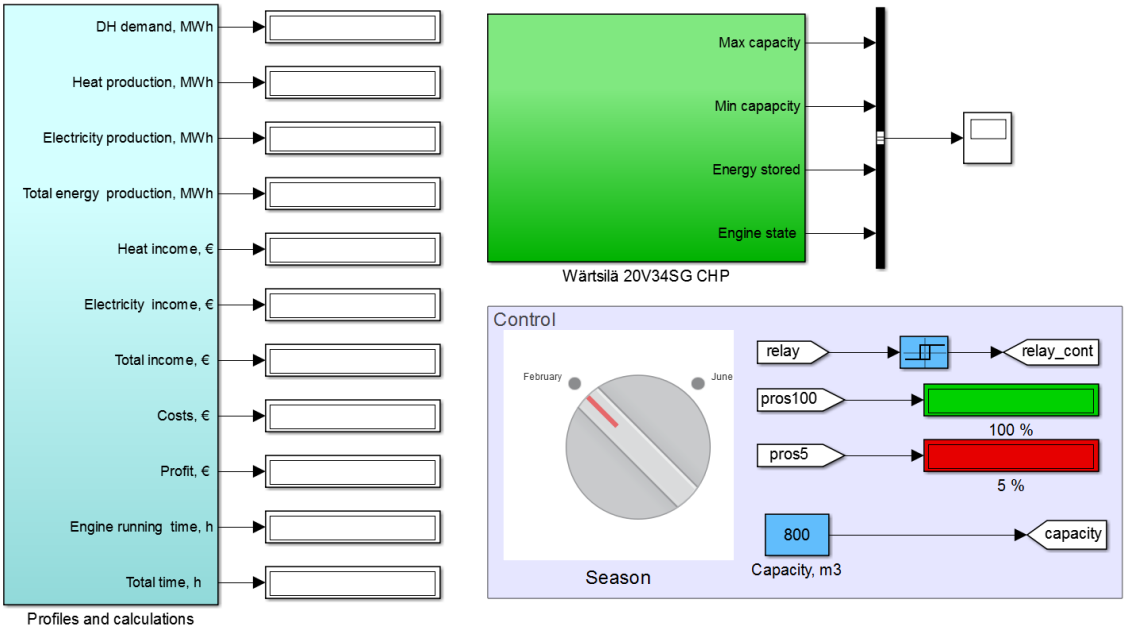

Figure 23. The top layer of the model in Case 2.

The top layer includes *Profiles and calculations* and *Wärtsilä 20V34SG CHP* subsystems and *Control* area. The limits for the accumulator capacity are set in *Control* area. *Profiles*

and calculations subsystem includes all the calculations to evaluate performance of the plant and functions to import the heat demand and electricity price profiles from MATLAB. *Profiles and calculations* subsystem is illustrated in Figure 24.

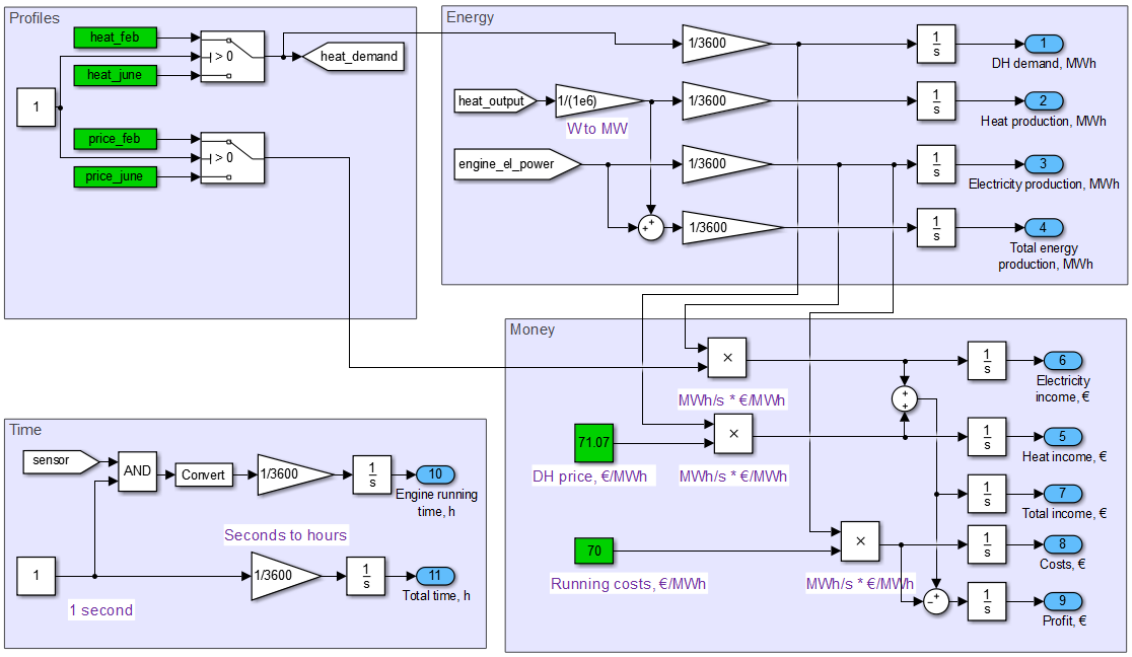

Figure 24. *Profiles and calculations* subsystem.

Profiles and calculations subsystem is divided into four areas. *Profiles* area imports the heat and electricity price profiles from MATLAB. A MATLAB script imports the values from Excel folder before executing the simulation. *Energy* area is in charge of all the calculations of energy demand or production. *Energy* area receives the information in watts or in mega-watts. These values are converted into megawatt-hours and then directed into the displays of the top layer. *Time* area indicates the time the engine was running and the total time of the simulation. *Money* area calculates the profit and the costs of the plant.

Wärtsilä 20V34SG CHP subsystem (Figure 25) includes the engine and the heat accumulator models.

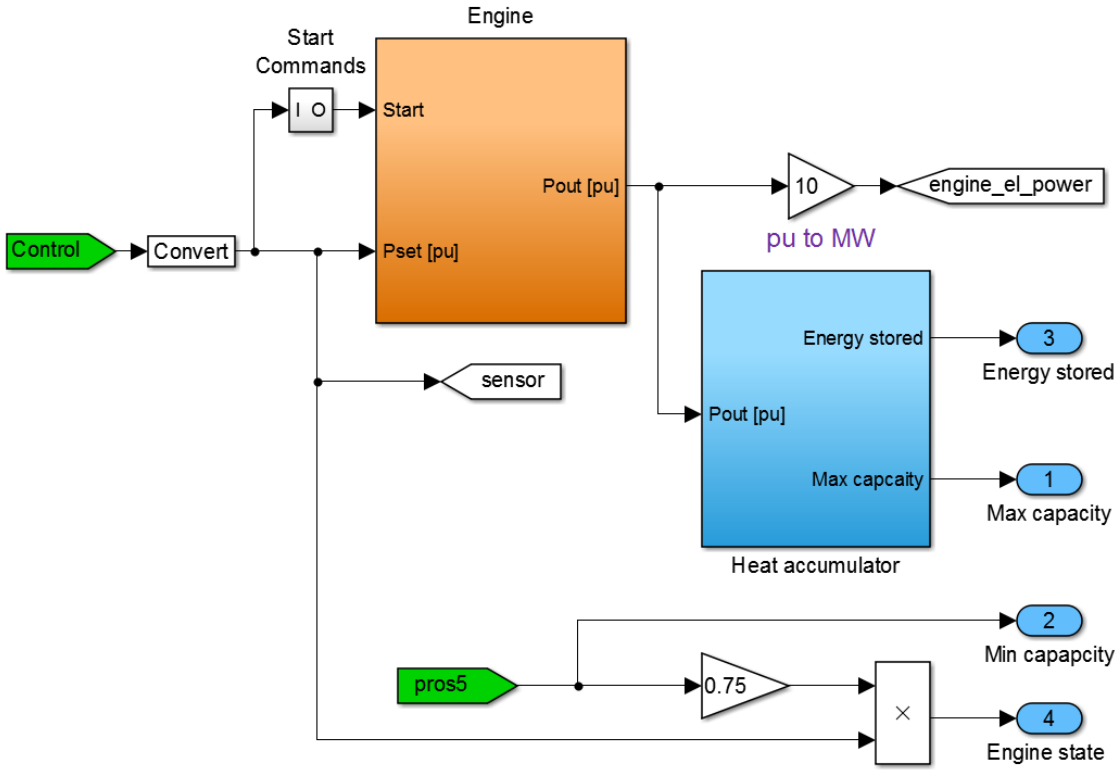

Figure 25. *Wärtsilä 20V34SG CHP* subsystem.

Engine subsystem consists of the simulation model provided by Wärtsilä. Its function is presented in the next section and the function of *Heat accumulator* subsystem is described after that.

5.2 Engine

Engine subsystem contains the function of the Wärtsilä 20V34SG gas engine. Any specific layout of that section is not described because the model is the property of Wärtsilä. However, the output of that model is presented in this section. The electricity output of the model is presented in Figure 26. It should be noted that the output of the simulation model differs from the output of the alternator of the real engine: 10 MW and 9.81 MW, respectively.

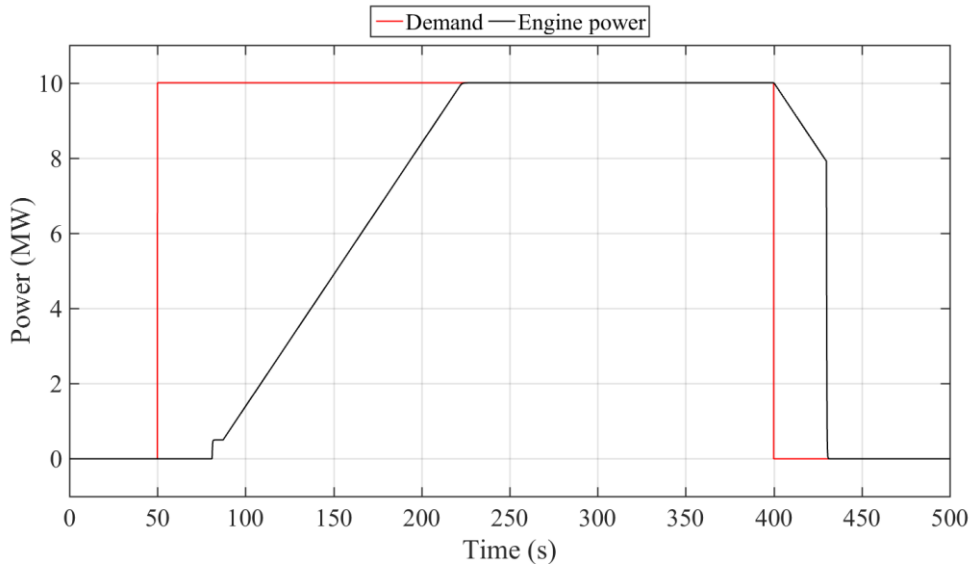

Figure 26. Electric power output of the model.

At the time 50 s, the electricity demand rises from 0 MW to 10 MW. Starting from that moment, the engine takes 30 s to complete startup-preparations, speed acceleration and synchronization to the electricity grid (Santoianni 2015: 12). After the startup-preparations, the engine starts to ramp up the power by 70 kW/s so the ramp rate is 4.2 MW/min. At the time 230 s, the engine reaches its maximum power and the full power stays on until 400 s. The engine starts to ramp down and after 30 s of ramping down the model sets the output to zero within few seconds.

The engine was assumed to be under hot start conditions in all of the simulations. Hot start means that the temperature of cooling water is maintained above 70 °C, engine and generator bearings are continuously prelubricated and the engine is slowly cycling (Santoianni 2015: 12). Cold start conditions were not considered in this thesis.

5.3 Heat accumulator

Heat accumulator subsystem covers the energy storage calculations (Figure 27).

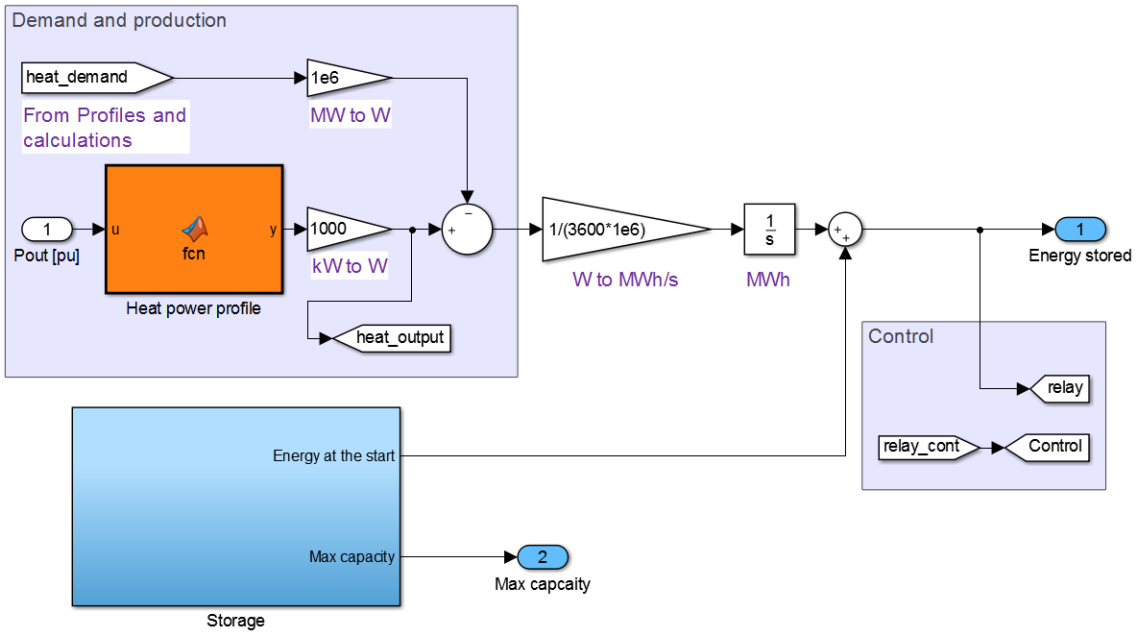

Figure 27. *Heat accumulator* subsystem.

Heat accumulator subsystem is divided into two areas and one subsystem. *Demand and production* area imports the heat demand profiles from *Profiles and calculations* subsystem. *Heat power profile* block includes a MATLAB script to describe heat production of the engine. Heat production is directly proportional to the electric output (Figure 28) and it is considered to start when the engine load is above 25-%.

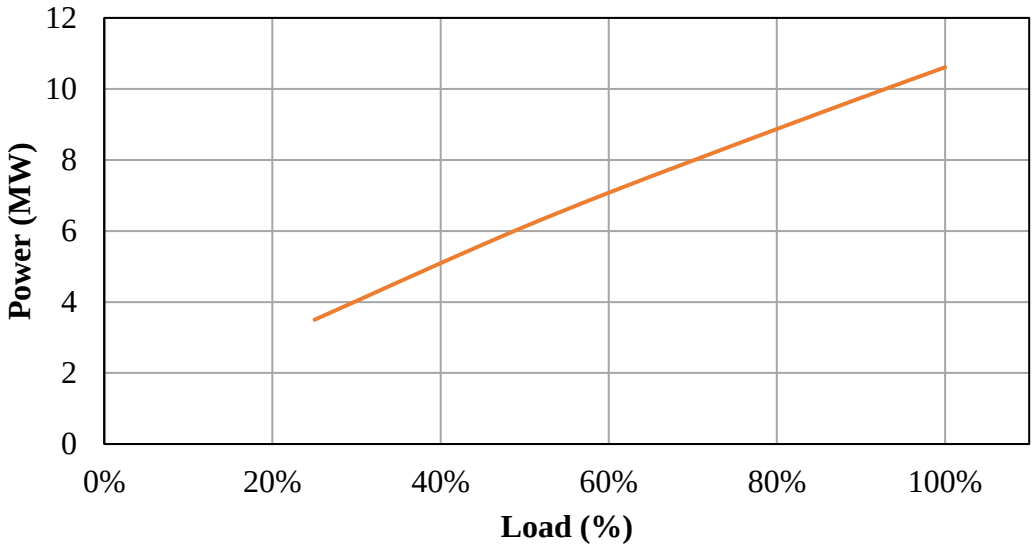

Figure 28. Heat production of the engine as a function of the load.

The heat demand is subtracted from the heat production in *Demand and production* area. This remaining heat power is then converted into megawatt-hours per second and then integrated to megawatt-hours. That value is then added to the initial amount of stored energy in the accumulator. During the times the engine is shut down, the heat accumulator keeps responding to the heat demand and the amount of energy in the accumulator is decreased. Respectively, when the engine is running, the amount of energy is increased in the accumulator. The increase is the energy deficit between the demand and supply.

Storage subsystem includes the heat accumulator capacity calculations. Layout of that subsystem is illustrated in Figure 29.

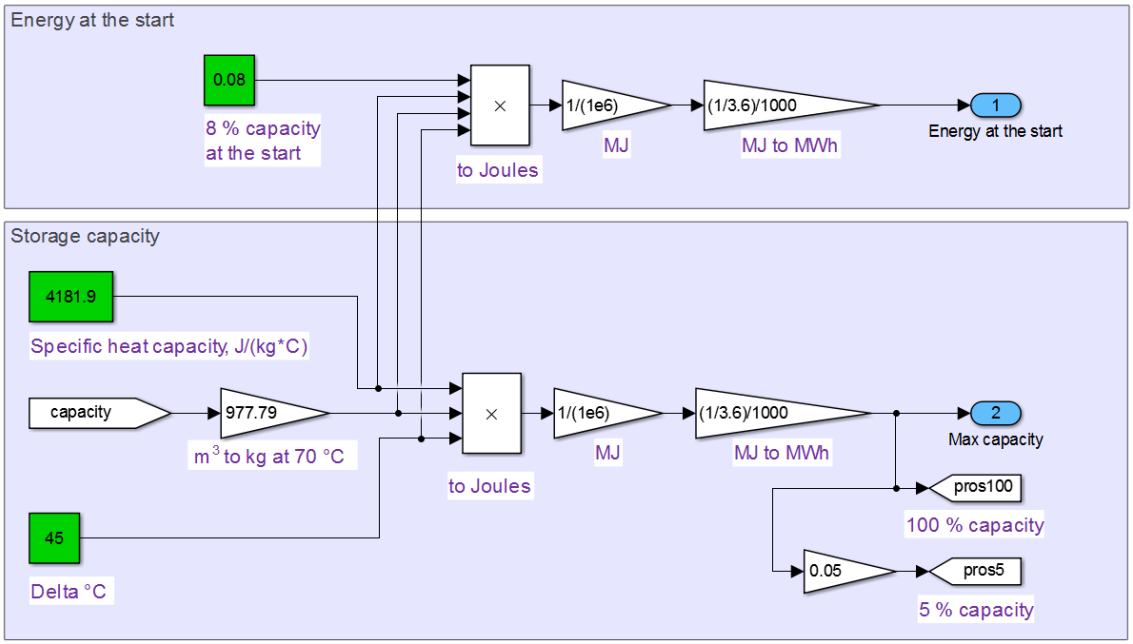

Figure 29. *Storage* subsystem.

Storage capacity area includes the maximum capacity of the heat accumulator for a certain volume. The specific heat capacity of water is 4181.9 J/(kg*K) and the temperature difference within the storage is 45 °C. The water density is 977.79 kg/m^3, taken at the temperature of 70 °C. *Capacity* value is transferred from the top layer. Of the maximum stored energy, 8-% is calculated in *Energy at the start* area and every heat mode simulation starts with this 8-% initial value. This value is then directed to the

previous layer, *Heat accumulator* subsystem. In that layer, either a positive or negative values of energy are added to the amount of stored energy at the start depending on whether the engine or the accumulator is responding to the heat demand.

5.4 Electric battery

The battery model is used in Cases 1 and 3. Layout of the battery model is shown in Figure 30.

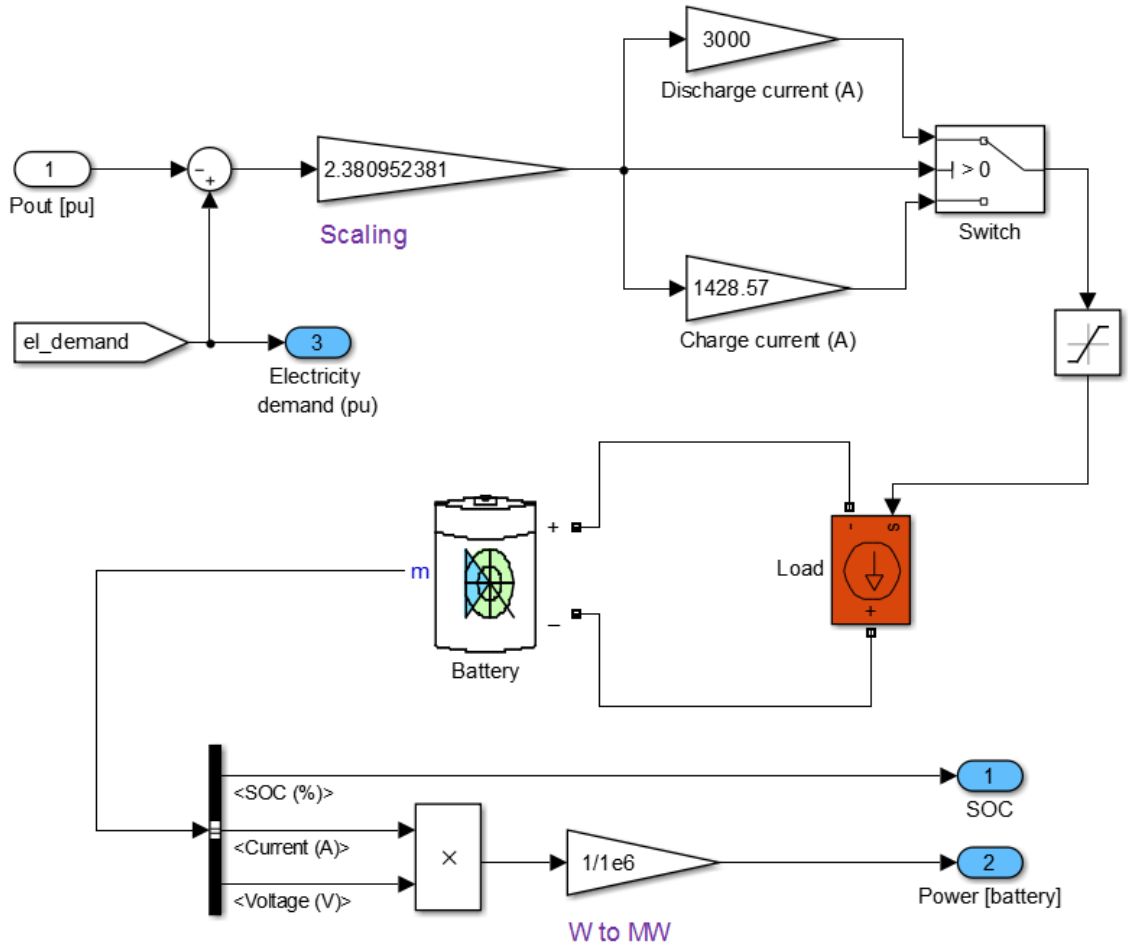

Figure 30. Layout of the battery model.

Pout block, which is the electrical output of the engine, is subtracted from the electricity demand block *el_demand.* This value expresses the difference between the demand and

supply in per-unit value. The value is scaled for the battery with *Scaling* block. *Scaling* block sets proper current for the load which lies in parallel with the *Battery* block. The current is always scaled to accommodate the difference between the demand and the supply: when the maximum difference occurs between the demand and supply, the battery is loaded with 3 000 A current for discharging and 1 400 A for charging. Three different parameters are routed from *Battery* block: SOC, current and voltage. Current and voltage signals are multiplied to form power. These values are directed to the previous layer.

Figure 31 illustrates the menu of *Battery* block. The menu shows the values used with the power output of 9.0 MW in Case 1.

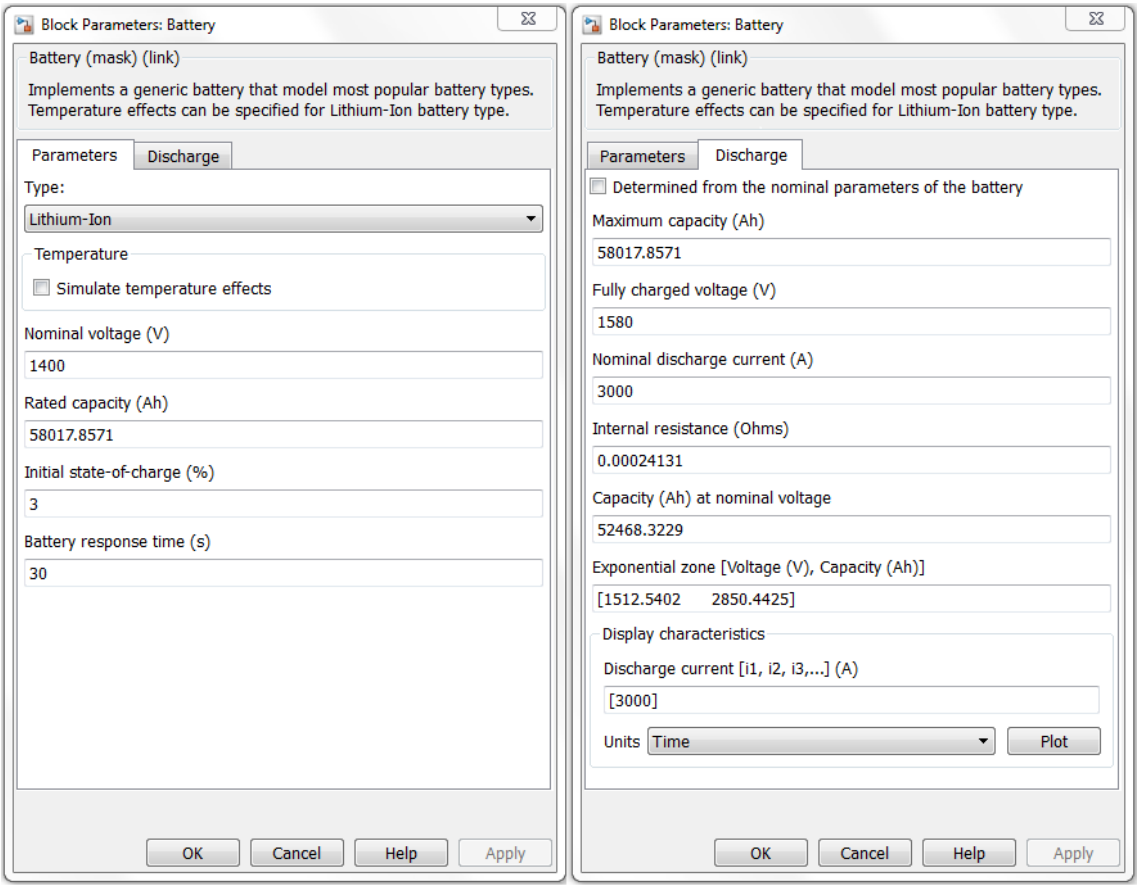

Figure 31. Parameters tab of *Battery* block.

6 RESULTS

Chapter 6 presents results of the simulations. The results of Case 1 show the proper battery capacity for every four fixed power outputs. The heat mode simulations present the most optimal heat accumulator capacities for Cases 2–4.

6.1 Electric mode - Case 1

The purpose of the electric mode simulations was to find a suitable and the smallest battery capacity for every four fixed engine power outputs. The smallest battery capacity would also mean the lowest price. The main prerequisites were that the battery had the ability to respond to changes in the electricity demand and to store excess energy. The battery capacity was determined by observing SOC. The aim was to scale the battery capacity so that SOC was kept between 0-% and 100-% throughout the whole simulation. Figures 32–35 illustrates the behavior of SOC with the four fixed engine outputs.

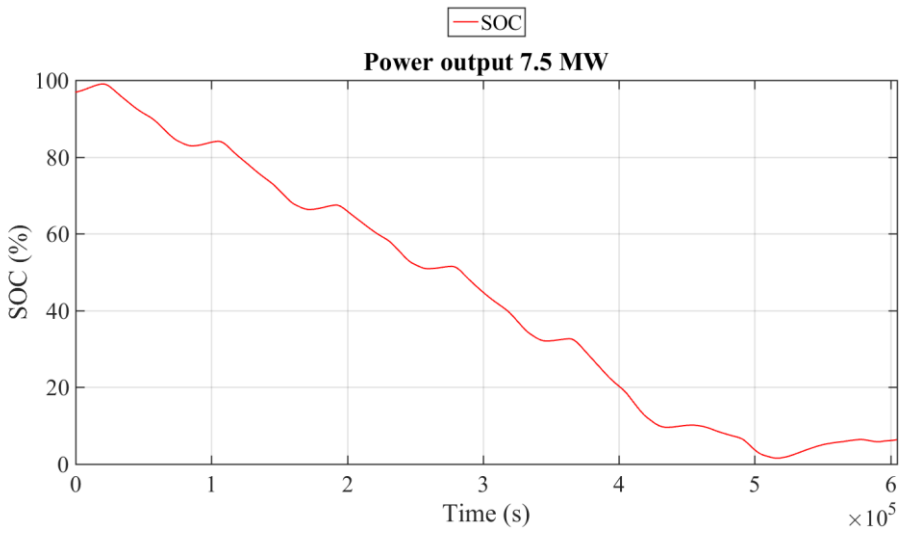

Figure 32. SOC with 7.5 MW power output.

With the power output of 7.5 MW, SOC dropped steadily during the week and settled approximately to 6.4-% by the end of the week. It should be borne in mind that the charging power was only approximately one half of the discharge power.

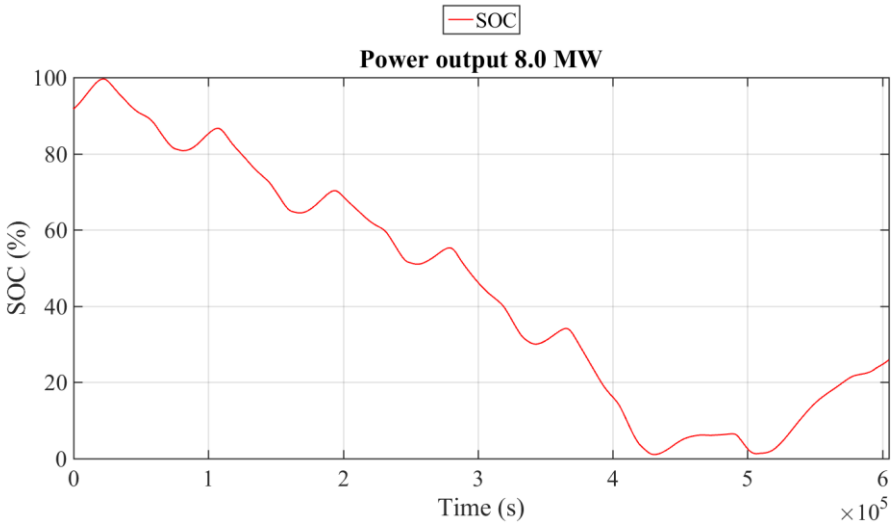

Figure 33. SOC with 8.0 MW power output.

With the power output of 8.0 MW, SOC dropped from initial 92-% close to 0-% but now the decrease varied more than at 7.5 MW output. SOC rose approximately to 26-% in the end of the week.

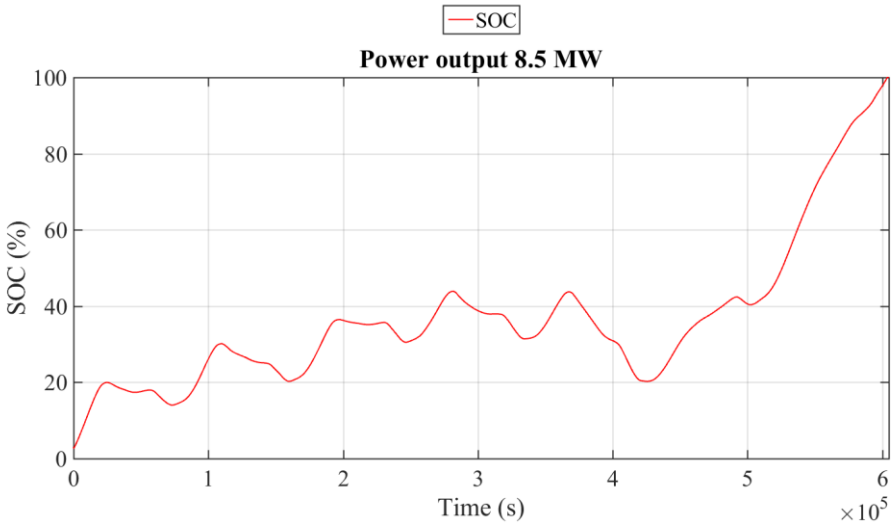

Figure 34. SOC with 8.5 MW power output.

The power output of 8.5 MW offered the most variable SOC curve. The initial value for SOC was 3-% and it fluctuated between the initial value and 40-% during the week. SOC rose to 100-% during the weekend.

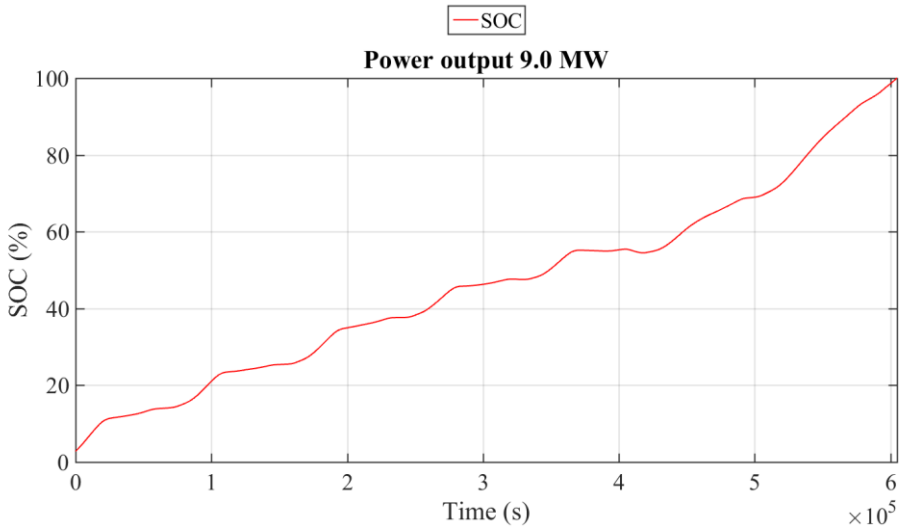

Figure 35. SOC with 9.0 MW power output.

With the 9.0 MW power output, the demand was almost all the time lower than the production. The battery started with a SOC of 3-% and by the end of the week it reached 100-%. With the two latter power outputs, the battery had to store the excess energy whereas at the first two outputs the required energy was mainly taken from the battery.

According to IRENA (2015: 30), the battery cell price for lithium-ion battery technology is predicted to be around 300 $/kWh by the year 2017. That value was used to calculate the price for every battery capacity and it was then converted to euros according to the currency rate provided by Bloomberg (2016) on 26th July 2016. The power output of 8.5 MW offered the smallest battery capacity. A 30 400 kWh battery resulted in the price of 8 300 000 €. The results of Case 1 are shown in Table 4.

Table 4. The results of Case 1.

Power output (MW)	Battery capacity (kWh)	Price (€)
7.5	109 250	29 784 609
8.0	47 500	12 949 830
8.5	30 400	8 287 891
9.5	81 225	22 144 209

6.2 Heat mode

In the rest of the cases, Cases 2, 3 and 4, heat production was prioritized over electricity production and decoupling was carried out with a heat accumulator. To begin with, the results of the plant operation is presented without a heat accumulator in Table 5. In these simulations, the engine ran with a 100-% load the whole week.

Table 5. The results of the simulations without a heat accumulator.

Season	Running costs, €/MWh	Heat income, €	Electricity income, €	Costs, €	Profit, €
February	70.00	81 098	57 950	117 580	21 468
	80.00	81 098	57 950	134 377	4 671
	90.00	81 098	57 950	151 175	-12 127
June	70.00	18 454	47 381	117 580	-51 745
	80.00	18 454	47 381	134 377	-68 542
	90.00	18 454	47 381	151 175	-85 340

The operation of the plant without a heat accumulator was shown to give some baseline for evaluating the results with a heat accumulator. The operation was profitable only during February with the running costs of 70 and 80 €/MWh. February with 90 €/MWh running costs and the whole June showed unprofitable operation.

The feasibility comparison between the tank volumes was made with an accumulator investment cost and profit of the plant. The accumulator investment cost was calculated with the following equation

$$400\ 000\ € + V * 33\ €, \tag{4}$$

where V is the volume of the heat accumulator (Hast, Rinne, Syri & Kiviluoma 2016: 5). The payback period of the tank, which is formed with the accumulator investment cost and profit of the plant, was calculated with the equation

$$payback\ period = \frac{accumulator\ investment\ cost}{\frac{profit}{52}} \tag{5}$$

The simulation time was one week. Consequently, the profit was achieved from a one-week operation. To give the payback period in years rather than week, the profit was divided by 52: the number of weeks in one year. In the results, the shortest payback period shows the most economical battery volume.

Tables of the results show necessary information to evaluate the operation of the plant. Heat accumulator volumes varied between 400 m^3 and 9 000 m^3 and the same volumes were used in every case. The electricity income, costs and the profit of the plant are presented. The heat income is not presented in the tables: it stays the same for each season. The heat income for February is 81 098 € and for June 18 454 €. The running costs of 70, 80 and 90 €/MWh were used. The running costs were given per electricity-MWh. In Case 4, the boiler costs were included as well. The engine running time indicates how many hours out of 168 hours (one week) the engine was running. The same information is provided for the boiler usage in Case 4. The most economical battery capacity is indicated by the rows with green color.

6.2.1 Case 2 - Simple operation method

Case 2 has the simplest operation method of all cases in the heat mode: the engine is only run to charge the heat accumulator. The results of the Case 2 simulations are presented in Tables 6–8.

Table 6. The results of Case 2 with 70 €/MWh running costs.

Season	Capacity, m3	Electricity income, €	Costs, €	Profit, €	Engine running time, h	Accumulator investment cost, €	Payback period, a
February	400	38 321	76 045	43 375	109.03	413 200	0.183
	800	37 867	76 456	42 510	109.43	426 400	0.193
	1 200	40 279	77 836	43 542	111.35	439 600	0.194
	1 600	38 610	77 570	42 139	110.92	452 800	0.207
	2 000	38 059	77 240	41 918	110.43	466 000	0.214
	2 500	38 438	76 165	43 371	108.89	482 500	0.214
	3 000	40 230	79 674	41 654	113.88	499 000	0.230
	4 000	38 966	78 497	41 567	112.18	532 000	0.246
	6 000	44 702	92 324	33 477	131.94	598 000	0.344
	9 000	47 505	90 861	37 743	129.82	697 000	0.355
June	400	9 135	18 191	9 398	26.23	413 200	0.846
	800	9 241	17 953	9 742	25.77	426 400	0.842
	1 200	8 060	17 602	8 912	25.23	439 600	0.949
	1 600	7 482	17 903	8 032	25.64	452 800	1.084
	2 000	6 819	23 253	2 020	33.28	466 000	4.437
	2 500	10 744	18 308	10 889	26.20	482 500	0.852
	3 000	7 505	22 008	3 950	31.48	499 000	2.429
	4 000	10 270	26 630	2 094	38.09	532 000	4.886
	6 000	8 901	20 965	6 390	29.97	598 000	1.800
	9 000	15 398	31 315	2 538	44.76	697 000	5.282

The most economical battery capacities were found to be 400 m^3 for February and 800 m^3 for June. The payback periods were 0.18 and 0.84 years, respectively. The results of February were quite straightforward: the payback period increased steadily as the volume increased. For June, the situation varied more. The reason for this may be due to more fluctuations in electricity prices and lower heat demand in June than in February: some of the accumulator volumes caused the engine to run mainly during the unprofitable times.

The following table illustrates the results of Case 2 with running costs of 80 €/MWh.

Table 7. The results of Case 2 with 80 €/MWh running costs.

Season	Capacity, m3	Electricity income, €	Costs, €	Profit, €	Engine running time, h	Accumulator investment cost, €	Payback period, a
February	400	38 321	86 909	32 511	109.03	413 200	0.244
	800	37 867	87 378	31 589	109.43	426 400	0.260
	1 200	40 279	88 955	32 422	111.35	439 600	0.261
	1 600	38 610	88 651	31 058	110.92	452 800	0.280
	2 000	38 059	88 274	30 884	110.43	466 000	0.290
	2 500	38 438	87 046	32 491	108.89	482 500	0.286
	3 000	40 230	91 056	30 272	113.88	499 000	0.317
	4 000	38 966	89 711	30 354	112.18	532 000	0.337
	6 000	44 702	105 513	20 288	131.94	598 000	0.567
	9 000	47 505	103 841	24 763	129.82	697 000	0.541
June	400	9 135	20 790	6 799	26.23	413 200	1.169
	800	9 241	20 518	7 177	25.77	426 400	1.143
	1 200	8 060	20 117	6 397	25.23	439 600	1.322
	1 600	7 482	20 461	5 475	25.64	452 800	1.591
	2 000	6 819	26 575	-1 302	33.28	466 000	
	2 500	10 744	20 923	8 274	26.20	482 500	1.121
	3 000	7 505	25 152	806	31.48	499 000	11.899
	4 000	10 270	30 434	-1 710	38.09	532 000	
	6 000	8 901	23 960	3 395	29.97	598 000	3.387
	9 000	15 398	35 788	-1 936	44.76	697 000	

The most suitable battery capacity was again 400 m^3 with the payback period of 0.24 years in February. For June, the most profitable capacity was 2 500 m^3 with payback period of 1.12 years. The simulations with heat demand in June showed partially unprofitable production. The same reason applied here than in the previous results with 70 €/MWh running costs: the electricity prices varied more and the heat demand was lower in June than in February.

The results with 90 €/MWh running costs are presented in Table 8.

Table 8. The results of Case 2 with 90 €/MWh running costs.

Season	Capacity, m3	Electricity income, €	Costs, €	Profit, €	Engine running time, h	Accumulator investment cost, €	Payback period, a
February	400	38 321	97 772	21 647	109.03	413 200	0.367
	800	37 867	98 300	20 666	109.43	426 400	0.397
	1 200	40 279	100 075	21 303	111.35	439 600	0.397
	1 600	38 610	99 733	19 976	110.92	452 800	0.436
	2 000	38 059	99 309	19 849	110.43	466 000	0.451
	2 500	38 438	97 926	21 610	108.89	482 500	0.429
	3 000	40 230	102 438	18 890	113.88	499 000	0.508
	4 000	38 966	100 925	19 140	112.18	532 000	0.535
	6 000	44 702	118 702	7 099	131.94	598 000	1.620
	9 000	47 505	116 821	11 783	129.82	697 000	1.138
June	400	9 135	23 388	4 200	26.23	413 200	1.892
	800	9 241	23 082	4 612	25.77	426 400	1.778
	1 200	8 060	22 631	3 883	25.23	439 600	2.177
	1 600	7 482	23 018	2 917	25.64	452 800	2.985
	2 000	6 819	29 897	-4 624	33.28	466 000	
	2 500	10 744	23 539	5 659	26.20	482 500	1.640
	3 000	7 505	28 296	-2 338	31.48	499 000	
	4 000	10 270	34 238	-5 514	38.09	532 000	
	6 000	8 901	26 955	400	29.97	598 000	28.740
	9 000	15 398	40 262	-6 409	44.76	697 000	

The most suitable heat accumulator volumes were found to be 400 m^3 with a payback period of 0.37 years for February and 2 500 m^3 with payback period of 1.64 years for June. The results of June showed the same kind of behavior than with the running costs of 80 €/MWh.

6.2.2 Case 3 - Profitability limit

Case 3 had more advanced operation method than Case 2. The engine was started in two events: the possible income of the plant exceeded the production costs or the stored energy dropped to 5-% of the maximum value. In the latter option, the engine charged the accumulator up to 10-% of the maximum capacity regardless of the production costs and shut down. Tables 9–11 present the results of Case 3.

Table 9. The results of Case 3 with 70 €/MWh production costs.

Season	Capacity, m3	Electricity income, €	Costs, €	Profit, €	Engine running time, h	Accumulator investment cost, €	Payback period, a
February	400	49 536	95 773	34 862	138.08	413 200	0.228
	800	48 649	93 533	36 215	134.20	426 400	0.226
	1 200	48 228	92 364	36 963	132.30	439 600	0.229
	1 600	47 774	91 124	37 749	130.43	452 800	0.231
	2 000	47 283	89 841	38 540	128.44	466 000	0.233
	2 500	46 599	88 088	39 610	125.96	482 500	0.234
	3 000	46 599	88 089	39 609	125.96	499 000	0.242
	4 000	46 599	88 088	39 610	125.96	532 000	0.258
	6 000	46 599	88 088	39 609	125.96	598 000	0.290
	9 000	46 599	88 088	39 610	125.96	697 000	0.338
June	400	13 663	22 967	9 150	35.44	413 200	0.868
	800	12 978	20 379	11 053	30.23	426 400	0.742
	1 200	12 648	19 141	11 961	28.00	439 600	0.707
	1 600	12 576	17 975	13 055	26.12	452 800	0.667
	2 000	12 089	16 940	13 603	24.55	466 000	0.659
	2 500	12 246	17 191	13 509	24.87	482 500	0.687
	3 000	12 421	16 999	13 876	24.55	499 000	0.692
	4 000	12 796	17 388	13 861	25.07	532 000	0.738
	6 000	12 652	17 248	13 858	24.83	598 000	0.830
	9 000	11 292	16 732	13 013	24.08	697 000	1.030

The most economical heat accumulator volume was now 800 m^3 for February and 2 000 m^3 for June. The payback periods were 0.23 and 0.66 years, respectively. However, the differences in the payback periods, for example in February, were minor. Extending the capacity above 2 000 m^3 had no influence on the profit in February. The profit rose to be slightly less than 14 000 € in June and enlarging the capacity only caused bigger accumulator investment costs.

The following table presents the results with 80 €/MWh running costs.

Table 10.The results of Case 3 with 80 €/MWh production costs.

Season	Capacity, m3	Electricity income, €	Costs, €	Profit, €	Engine running time, h	Accumulator investment cost, €	Payback period, a
February	400	43 887	94 792	30 194	121.38	413 200	0.263
	800	41 534	88 086	34 547	111.37	426 400	0.237
	1 200	40 748	86 068	35 779	108.44	439 600	0.236
	1 600	40 752	85 921	35 930	108.11	452 800	0.242
	2 000	40 798	86 106	35 791	108.23	466 000	0.250
	2 500	40 749	85 977	35 871	107.97	482 500	0.259
	3 000	40 175	85 850	35 424	107.77	499 000	0.271
	4 000	40 784	85 858	36 025	107.69	532 000	0.284
	6 000	40 870	86 221	35 748	108.08	598 000	0.322
	9 000	40 555	85 509	36 145	107.16	697 000	0.371
June	400	6 822	19 517	5 758	28.32	413 200	1.380
	800	6 814	19 490	5 778	26.38	426 400	1.419
	1 200	6 671	19 439	5 686	25.65	439 600	1.487
	1 600	6 872	19 565	5 761	25.53	452 800	1.512
	2 000	6 810	19 636	5 627	25.36	466 000	1.593
	2 500	6 771	19 745	5 480	25.35	482 500	1.693
	3 000	6 540	19 287	5 707	24.69	499 000	1.681
	4 000	6 822	19 201	6 075	24.43	532 000	1.684
	6 000	6 150	18 876	5 727	23.90	598 000	2.008
	9 000	6 124	19 682	4 897	24.81	697 000	2.737

When operating with 80 €/MWh running costs, the most optimal accumulator volumes were 1 200 m^3 for February and 400 m^3 for June. The payback periods were 0.24 and 1.38 years, respectively. Yet again, the differences for February were rather small. For June, the results presented rather diverse optimum for the accumulator volume than the previous simulations did with 70 €/MWh running costs. The reason for this was higher running costs. Now the costs were more aligned than they were with 70 €/MWh running costs: the plant running costs for every accumulator volume were approximately 19 600 € with few exceptions. This showed that the smallest steel tank storage was the most suitable option.

Table 11 illustrates the results with 90 €/MWh running costs.

Table 11. The results of Case 3 with 90 €/MWh production costs.

Season	Capacity, m3	Electricity income, €	Costs, €	Profit, €	Engine running time, h	Accumulator investment cost, €	Payback period, a
February	400	41 060	99 428	22 731	114.48	413 200	0.350
	800	40 250	97 032	24 318	109.96	426 400	0.337
	1 200	40 180	96 853	24 426	109.12	439 600	0.346
	1 600	40 132	96 564	24 666	108.49	452 800	0.353
	2 000	40 079	96 603	24 574	108.33	466 000	0.365
	2 500	40 238	96 928	24 408	108.52	482 500	0.380
	3 000	40 260	96 970	24 388	108.49	499 000	0.393
	4 000	40 277	96 716	24 660	108.02	532 000	0.415
	6 000	40 252	96 861	24 490	108.06	598 000	0.470
	9 000	40 134	96 837	24 395	107.97	697 000	0.549
June	400	6 829	21 969	3 314	28.32	413 200	2.398
	800	6 806	21 910	3 350	26.38	426 400	2.448
	1 200	6 677	21 867	3 264	25.65	439 600	2.590
	1 600	6 875	22 030	3 298	25.53	452 800	2.640
	2 000	6 805	22 045	3 214	25.36	466 000	2.788
	2 500	6 762	22 183	3 033	25.35	482 500	3.060
	3 000	6 555	21 752	3 256	24.69	499 000	2.947
	4 000	6 840	21 706	3 588	24.43	532 000	2.851
	6 000	6 150	21 236	3 367	23.90	598 000	3.415
	9 000	6 124	22 142	2 436	24.81	697 000	5.502

The most economical capacity was 800 m^3 with the payback period of 0.34 years for February and 400 m^3 with the payback period of 2.40 years for June. Compared to 80 €/MWh running costs, the most suitable accumulator capacity for June remains the same. For February, the most optimal capacity was one volume step smaller.

Case 3 had also a battery variant. The simulations showed that the suitable battery capacity was 300 kWh. This resulted in a price of 81 584 €. Compared to Case 1, the battery capacity was now very much smaller because the battery smooths only the ramp-ups and -downs.

6.2.3 Case 4 - Electric boiler

Case 4 had the same operation method than Case 3. The only exception was that now an electric boiler heats the DH water when the accumulator emptied and it was not profitable to run the engine. The results of this Case are presented in Tables 12–14.

Table 12. The results of Case 4 with 70 €/MWh production costs.

Season	Capacity, m3	Electricity income, €	Boiler costs, €	Costs, €	Profit, €	Engine running time, h	Boiler running time, h	Accumulator investment cost, €	Payback period, a
February	400	46 599	3 111	91 199	36 498	125.96	25.81	413 200	0.218
	800	46 599	2 172	90 261	37 437	125.96	19.09	426 400	0.219
	1 200	46 599	1 681	89 769	37 929	125.96	13.53	439 600	0.223
	1 600	46 599	1 177	89 268	38 430	125.96	9.06	452 800	0.227
	2 000	46 599	656	88 744	38 954	125.96	4.90	466 000	0.230
	2 500	46 600	0	88 091	39 608	125.96	0.00	482 500	0.234
	3 000	46 599	0	88 088	39 610	125.96	0.00	499 000	0.242
	4 000	46 599	0	88 088	39 610	125.96	0.00	532 000	0.258
	6 000	46 599	0	88 088	39 610	125.96	0.00	598 000	0.290
	9 000	46 599	0	88 088	39 610	125.96	0.00	697 000	0.338
June	400	10 461	3 471	15 450	13 465	17.20	113.18	413 200	0.590
	800	10 461	2 707	14 686	14 229	17.20	91.36	426 400	0.576
	1 200	10 461	2 389	14 368	14 547	17.20	79.71	439 600	0.581
	1 600	10 461	2 120	14 099	14 816	17.20	68.99	452 800	0.588
	2 000	10 462	1 937	13 916	14 999	17.20	63.45	466 000	0.597
	2 500	10 461	1 929	13 908	15 008	17.20	62.71	482 500	0.618
	3 000	10 461	1 920	13 900	15 016	17.20	61.97	499 000	0.639
	4 000	10 462	1 904	13 883	15 032	17.20	60.57	532 000	0.681
	6 000	10 461	1 797	13 776	15 139	17.20	57.14	598 000	0.760
	9 000	10 461	1 518	13 497	15 418	17.20	52.58	697 000	0.869

The most optimal battery capacity was 400 m^3 for February and 800 m^3 for June with 70 €/MWh running costs. The payback periods were 0.22 and 0.58 years, respectively. The boiler was not started with capacities over 2 000 m^3 in February. The electricity income was the same in February and June because the engine ran for the same time in both of the cases.

Table 13 illustrates the results with 80 €/MWh running costs.

Table 13. The results of Case 4 with 80 €/MWh production costs.

Season	Capacity, m3	Electricity income, €	Boiler costs, €	Costs, €	Profit, €	Engine running time, h	Boiler running time, h	Accumulator investment cost, €	Payback period, a
February	400	34 891	9 595	78 503	37 487	86.30	63.01	413 200	0.212
	800	34 891	7 069	75 976	40 013	86.30	47.92	426 400	0.205
	1 200	34 891	6 264	75 171	40 818	86.30	43.59	439 600	0.207
	1 600	34 891	6 248	75 055	40 935	86.30	43.51	452 800	0.213
	2 000	34 891	6 231	75 138	40 851	86.30	43.43	466 000	0.219
	2 500	34 891	6 211	75 118	40 871	86.30	43.32	482 500	0.227
	3 000	34 891	6 190	75 098	40 892	86.30	43.22	499 000	0.235
	4 000	34 891	6 150	75 057	40 932	86.30	43.02	532 000	0.250
	6 000	34 891	6 068	74 976	41 014	86.30	42.61	598 000	0.280
	9 000	34 891	5 947	74 854	41 135	86.30	42.00	697 000	0.326
June	400	0	7 318	7 318	11 136	0.00	167.28	413 200	0.714
	800	0	7 311	7 311	11 143	0.00	166.63	426 400	0.736
	1 200	0	7 304	7 304	11 150	0.00	166.05	439 600	0.758
	1 600	0	7 297	7 297	11 157	0.00	165.48	452 800	0.780
	2 000	0	7 291	7 291	11 163	0.00	164.90	466 000	0.803
	2 500	0	7 282	7 282	11 171	0.00	164.16	482 500	0.831
	3 000	0	7 274	7 274	11 180	0.00	163.42	499 000	0.858
	4 000	0	7 257	7 257	11 196	0.00	162.02	532 000	0.914
	6 000	0	7 150	7 150	11 303	0.00	158.59	598 000	1.017
	9 000	0	6 862	6 862	11 591	0.00	154.98	697 000	1.156

With 80 €/MWh running costs, the most economical volume was 800 m^3 with 0.21 years payback period for February. The heat demand of June showed that a 400 m^3 tank was the most suitable and the payback period for that was 0.71 years. It should be noted that during June, only the heat boiler was used. As mentioned in Chapter 4.2.2, the income of the electricity and heat did not exceed the running costs at any point. This was caused by the low heat demand which affected the total income.

Table 14 presents the results with running costs of 90 €/MWh.

Table 14. The results of Case 4 with 90 €/MWh production costs.

Season	Capacity, m3	Electricity income, €	Boiler costs, €	Costs, €	Profit, €	Engine running time, h	Boiler running time, h	Accumulator investment cost, €	Payback period, a
February	400	26 611	15 448	70 043	37 667	60.86	90.96	413 200	0.211
	800	26 608	14 571	69 155	38 551	60.85	86.36	426 400	0.213
	1 200	26 608	14 497	69 081	38 625	60.86	85.99	439 600	0.219
	1 600	26 608	14 481	69 064	38 642	60.86	85.91	452 800	0.225
	2 000	26 608	14 464	69 048	38 658	60.86	85.82	466 000	0.232
	2 500	26 609	14 443	69 031	38 677	60.86	85.72	482 500	0.240
	3 000	26 609	14 422	69 010	38 698	60.86	85.62	499 000	0.248
	4 000	26 608	14 381	68 965	38 741	60.86	85.41	532 000	0.264
	6 000	26 608	14 299	68 883	38 823	60.86	85.01	598 000	0.296
	9 000	26 608	14 177	68 762	38 945	60.86	84.39	697 000	0.344
June	400	0	7 318	7 318	11 136	0.00	167.28	413 200	0.714
	800	0	7 311	7 311	11 143	0.00	166.63	426 400	0.736
	1 200	0	7 304	7 304	11 150	0.00	166.05	439 600	0.758
	1 600	0	7 297	7 297	11 157	0.00	165.48	452 800	0.780
	2 000	0	7 291	7 291	11 163	0.00	164.90	466 000	0.803
	2 500	0	7 282	7 290	11 163	0.00	164.16	482 500	0.831
	3 000	0	7 274	7 274	11 180	0.00	163.42	499 000	0.858
	4 000	0	7 257	7 257	11 196	0.00	162.01	532 000	0.914
	6 000	0	7 150	7 151	11 303	0.00	158.59	598 000	1.017
	9 000	0	6 862	6 862	11 591	0.00	154.98	697 000	1.156

The most feasible battery capacity was 400 m^3 for both February and June. The payback periods were 0.21 and 0.71 years, respectively. As with 80 €/MWh running costs, the income of the plant did not rise above the running costs during June and only the heat boiler was used the whole week.

Table 15 sums up the most economical heat accumulator volumes and payback periods from all of the cases. To start with running costs of 70 €/MWh, it was surprising that Case 2 offered the shortest payback period in February. In Case 2, the engine ran purely based on heat accumulator status and it did not observe the profitability of the plant. The reason for feasible operation in Case 2 may be that the engine accidentally runs during the high electricity price periods and stands idle during the low price periods. However, this changes for June. Now the shortest payback period was in Case 4 and Case 2 offered the longest payback period with 70 €/MWh running costs.

Table 15. The most optimal heat accumulator volumes in Cases 2, 3 and 4.

February	Running costs, €/MWh	Capacity, m3	Payback period, a	June	Running costs, €/MWh	Capacity, m3	Payback period, a
Case 2	70.00	400	0.183	Case 2	70.00	800	0.842
	80.00	400	0.244		80.00	2 500	1.121
	90.00	400	0.367		90.00	2 500	1.640
Case 3	70.00	800	0.226	Case 3	70.00	2 000	0.659
	80.00	1 200	0.236		80.00	400	1.380
	90.00	800	0.337		90.00	400	2.398
Case 4	70.00	400	0.218	Case 4	70.00	800	0.576
	80.00	800	0.205		80.00	400	0.714
	90.00	400	0.211		90.00	400	0.714

In June, the income of the plant didn't rise above the profitability limit with the running costs of 80 and 90 €/MWh. In Case 3, stored energy in the heat accumulator fluctuated between 5-% and 10-% of the maximum capacity because the engine runs unprofitable throughout the simulations when it has to charge the accumulator. In Case 4, only the electric boiler heats the district heating water and the accumulator was not loaded. Therefore, the results of these simulations, Case 3 and 4 with running costs of 80 and 90 €/MWh in June, can be ignored because the aim was to study the behavior of engine power plants with a heat accumulator. Taking these into consideration, the most suitable battery volumes are between 800 m^3 and 2 500 m^3 for June. Optimal storage volumes for February are between 400 m^3 and 1 200 m^3.

7 CONCLUSIONS AND RECOMMENDATIONS

Four different cases were studied to find out, how the decoupling of electricity and heat production of a gas engine driven CHP plant can be most favorably realized. The cases comprised the electric and heat modes. The electric mode studied smoothing of fluctuations in the electricity demand by means of a lithium-ion battery. The heat mode compared the operation of the plant with different heat accumulator volumes, running costs and heat demands.

Based on the simulations results of the built operating models, the following conclusions could be drawn:

- In the electric mode, the power output of 8.5 MW out of 7.5, 8.0, 8.5 and 9.0 MW offered the smallest battery capacity: A 30 400 kWh lithium-ion battery resulted in a price of 8.3 million euros.
- The price is quite high for smoothing fluctuations, not to mention to decouple the whole production.
- A lithium-ion battery with the capacity of 300 kWh was able to smooth the power output of the engine during ramp-ups and -downs.
- The heat accumulator made the production more profitable compared to the plant without one.
- In the heat mode, it was more economical to utilize smaller heat accumulator volumes in the winter (400–1 200 m^3) than in the summer (800–2 500 m^3).
- The average electricity price and heat demand were lower in the summer than in the winter which affected on the optimal accumulator volumes.

For future studies, it is recommended to incorporate longer electricity and heat demands. The period of one-week was quite short time for simulations. It would be advantageous to prolong the heat demand to last for a whole year. This way differences in summer and winter demands are taken into account.

8 SUMMARY

This thesis was carried out within the research program Flexible Energy Systems and the target of the program was to create novel technological and business concepts enhancing the transition from the current energy systems towards sustainable systems. Gas engine driven power plants may play an important role in sustainable systems in the future. The plant with fast ramp-ups and -downs operates well in a system with increasing share of renewables. Flexibility enables the plant to run during high electricity price periods and the heat accumulator is able to meet the heat demand during low electricity prices.

The aim of this thesis was to study possibilities to decouple heat and electricity production in an engine driven CHP plant with energy storage solutions. The target was to compare heat accumulator volumes in a CHP plant which consisted of one Wärtsilä 20V34SG gas engine and a heat accumulator. The performance of the plant was evaluated at different operation methods, heat demands and running costs. An electric battery was studied in case of smoothing fluctuations in the electricity demand.

The theory part of the thesis presented the principle of an engine driven CHP plant, a heat accumulator and an electric battery. The Simulink simulation models were constructed to conduct the simulations which were divided into two modes. The electric mode simulations studied the plant operation with an electric battery and the heat mode with a heat accumulator.

In the electric mode, the plant was loaded with a fluctuating electricity demand. The plant was run with four fixed power outputs: 7.5, 8.0, 8.5 and 9.0 MW. The capacity of the battery was scaled for every power output. The power output of 8.5 MW offered the smallest and the cheapest battery capacity. The battery capacity of 30 400 kWh resulted in a price of 8.3 million euros. The heat mode compared heat accumulator volumes at different operation methods, running costs (70, 80 and 90 €/MWh) and heat demands (winter and summer). The simulations showed that it was more profitable to utilize smaller heat accumulator volumes in the winter (400–1 200 m^3) than in the summer (800–2 500 m^3).

In the simulations, one-week energy demand profiles were used: the capacity of the lithium-ion battery and optimal volumes of the heat accumulators were found with this time period. It should be noted that a one-week period is rather short time for conducting realistic simulations dealing with energy storages. Therefore, in future studies, it is highly recommended to use longer energy demand periods. This way, for example, seasonal differences in heat demand are taken into account.

REFERENCES

Abraham D.P., M.M. Furczon, S.-H. Kang, D.W. Dees & A.N. Jansen (2008). Effect of electrolyte composition on initial cycling and impedance characteristics of lithium-ion cells. *Journal of Power Sources,* volume 180, 612–620. Ed. Stefano Passerini. ISSN: 0378-7753.

Bloomberg (2016). EURUSD Spot Exchange Rate [online]. [Cited 26.7.2016]. Available in: http://www.bloomberg.com/quote/EURUSD:CUR

Campos Celador, A., M. Odriozola & J.M. Sala (2010). Implications of the modelling of stratified hot water storage tanks in the simulation of CHP plants. *Energy Conversion and Management,* volume 52, issues 8–9, 3018–3026. Ed. Moh'd Ahmad Al-Nimr. ISSN: 0196-8904.

Energiateollisuus (2006). *Kaukolämmön käsikirja* [in Finnish]. 1. edition. Helsinki: Adato Energia. 566 p. ISBN 952-5615-08-1.

Energiateollisuus (2016a). Kaukolämmön toimintaperiaate [in Finnish] [online]. [Cited 1.8.2016]. Available in: http://energia.fi/koti-ja-lammitys/kaukolammitys/toimintaperiaate

Energiateollisuus (2016b). Kaukolämmön hinnat tyyppitaloissa eri paikkakunnilla [in Finnish] [online]. [Cited 19.7.2016]. Available in: http://energia.fi/tilastot/kaukolammon-hinnat-tyyppitaloissa-eri-paikkakunnilla

Fingrid (2016a). Power System in Finland [online]. [Cited 8.8.2016]. Available in: http://www.fingrid.fi/en/powersystem/general%20description/Power%20System%20in%20Finland/Pages/default.aspx

Fingrid (2016b). Load and generation [online]. [Cited 19.9.2016]. Available in: http://www.fingrid.fi/EN/ELECTRICITY-MARKET/LOAD-AND-GENERATION/Pages/default.aspx

Garcia, N. P., K. Vatopoulos, A. K. Riekkola, A. P. Lopez & L. Olsen (2012). Best available technologies for the heat and cooling market in the European Union [online]. Luxemburg: Publications Office of the European Union, 2012. ISBN 978-92-79-25608-0.

Haga N., V. Kortela & A. Ahnger (2012). Smart Power Generation – District heating solutions [online]. 24 p. [Cited 2.8.2016]. Available in: http:// www.wartsila.com/docs/default-source/Power-Plants-documents/downloads/ White-papers/general/Smart-Power-Generation-District-heating-solutions.pdf

Hast, A., S. Rinne, S. Syri & J. Kiviluoma (2016). The role of heat storages in facilitating the adaptation of DH systems to large amount of variable RES electricity [Electronic publication]. *The 29th international conference on efficiency, cost, optimization, simulation and environmental impact of energy systems. June 19–23, 2016, Portorož, Slovenia.*

Huhtinen, M., R. Korhonen, T. Pimiä & S. Urpalainen (2013). Voimalaitostekniikka [in Finnish]. 2. ed. Helsinki: Opetushallitus. 344 p. ISBN 978-952-13-5426-7.

IRENA (2013). Thermal Energy Storage - Technology Brief [online]. 22 p. [Cited 3.8.2016]. Available in: https://www.irena.org/DocumentDownloads/ Publications/IRENA-ETSAP%20Tech%20Brief%20E17%20Thermal% 20Energy%20Storage.pdf

IRENA (2015). Battery storage for renewables: market status and technology outlook [online]. 54 p. [Cited 25.7.2016]. Available in: http://www.irena.org/ DocumentDownloads/Publications/IRENA_Battery_Storage_report_2015.pdf

Karlsson, J. & S. Gray (2008). Modularity and flexibility in Wärtsilä Power plants [online]. *Twentyfour7*, issue 1/2008, 78 p. Available in: http:// www.twentyfour7magazine.com/en/archive/

Li, G (2016). Sensible heat thermal storage energy and exergy performance evaluations. *Renewable and Sustainable Energy Reviews 53*, 897–923. Ed. Lawrence Kazmerski. ISSN: 1364-0321.

MathWorks (2016). Simulink [online]. [Cited 5.7.2016]. Available in: http:// se.mathworks.com/products/simulink/

Nitta N., F. Wu, J. T. Lee & G. Yushin (2015). Li-ion battery materials: present and future. *Materials Today*, volume 18, issue 5, 252–264. Ed. S. Bland. ISSN: 1369-7021.

Njoku, H.O., O.V. Ekechukwu & S.O. Onyegegbu (2015). Comparison of energy, exergy and entropy generation-based criteria for evaluating stratified thermal store performances. *Energy and Buildings*, volume 124, 141-152. Eds. Jianlei Niu & Mattheos Santamouris. ISSN: 0378-7788.

Nord Pool (2016). The power market [online]. [Cited 15.8.2016]. Available in: http:// www.nordpoolspot.com/How-does-it-work/

Park, M., X. Zhang, M. Chung, G. B. Less & A. M. Sastry (2010). A review of conduction phenomena in Li-ion batteries. *Journal of Power Sources 195*, 7904–7929. Ed. Stefano Passerini. ISSN: 0378-7753.

Saft (2015). Intensium Max [online]. 8 p. [Cited 4.8.2016]. Available in: http:// www.saftbatteries.com/battery-search/intensium%C2%AE-max

Santoianni, D. (2015). Defining true flexibility – a comparison of gas-fired power generating technologies [online]. *Wärtsilä Technical Journal In Detail*, 2015: 1, 10–15. [Cited 5.7.2016]. Available in: http://www.indetailmagazine.com/en/

Spanggaard, M. & T. Schwaner (2013). Basics of Thermal Stratification [online]. 10 p. [Cited 27.7.2016]. Available in: http://eyecular.com/wp-content/uploads/2013/06/Thermal-stratification-v11.pdf

Wärtsilä (2010). Combined Heat and Power [online]. 16 p. [Cited 9.8.2016]. Available in: http://www.cogeneurope.eu/medialibrary/2011/09/30/3476a559/Combined%20Heat%20and%20Power.pdf

Wärtsilä (2013). Combined Cooling, Heating and Power [online]. 12 p. [Cited 29.7.2016]. Available in: http://cdn.wartsila.com/docs/default-source/Power-Plants-documents/reference-documents/brochures/combined_cooling_heating_and_power-2013.pdf

Wärtsilä (2014). Gas and multi-fuel power plants [online]. 12 p. [Cited 1.8.2016]. Available in: http://cdn.wartsila.com/docs/default-source/Power-Plants-documents/reference-documents/brochures/gas-and-multi-fuel-power-plants-2014.pdf

Wärtsilä (2016a). Dynamic District Heating - A technical guide for a flexible CHP plant [online]. 12 p. [Cited 29.7.2016]. Available in: http://cdn.wartsila.com/docs/default-source/Power-Plants-documents/downloads/brochures/dynamic-district-heating---a-technical-guide_v2.pdf

Wärtsilä (2016b). Wärtsilä 34SG – Engine generating set [online]. 2 p. [Cited 2.8.2016]. Available in: http://cdn.wartsila.com/docs/default-source/Power-Plants-documents/downloads/product-leaflets/w34sg_leaflet.pdf